

REPRODUCTION
COPY
IS-4 REPORT SECTION

C. 3

*Reactivity Effects of Void Formations
in a Solution Critical Assembly*

Los Alamos
NATIONAL LABORATORY

*Los Alamos National Laboratory is operated by the University of California
for the United States Department of Energy under contract W-7405-ENG-36.*

LOS ALAMOS NATIONAL LABORATORY



3 9338 00208 9661

This thesis was accepted by the Department of Nuclear Engineering, North Carolina State University, Raleigh, North Carolina, in partial fulfillment of the requirements for the degree of Master of Nuclear Engineering. The text and illustrations are the independent work of the author and only the front matter has been edited by the IS-1 staff to conform with Department of Energy and Los Alamos National Laboratory publication policies.

An Affirmative Action/Equal Opportunity Employer

This report was prepared as an account of work sponsored by an agency of the United States Government. Neither The Regents of the University of California, the United States Government nor any agency thereof, nor any of their employees, makes any warranty, express or implied, or assumes any legal liability or responsibility for the accuracy, completeness, or usefulness of any information, apparatus, product, or process disclosed, or represents that its use would not infringe privately owned rights. Reference herein to any specific commercial product, process, or service by trade name, trademark, manufacturer, or otherwise, does not necessarily constitute or imply its endorsement, recommendation, or favoring by The Regents of the University of California, the United States Government, or any agency thereof. The views and opinions of authors expressed herein do not necessarily state or reflect those of The Regents of the University of California, the United States Government, or any agency thereof.

LA-12716-T
Thesis

UC-714
Issued: January 1994

*Reactivity Effects of Void Formations
in a Solution Critical Assembly*

*Steven G. Walters**

**Staff Research Assistant at Los Alamos Group N-2.*





ACKNOWLEDGMENTS

I would like to express thanks and appreciation to Dr. Dudziak for his patience and support. The ideas that he contributed have led to an extremely enjoyable and enlightening project.

The primary group at Los Alamos National Laboratory that aided in this project was the Advanced Nuclear Technology group (N-2). This group provided an ideal location, and the equipment necessary to perform my research. Within the group, I would like to thank Ken Butterfield for providing insight into the project as well as allowing me the freedom to learn from my own mistakes.

I would like to thank X-6 for allowing me the use of THREEDANT. The experience of using this discrete-ordinates code in direct contrast to MCNP has been truly enlightening. In particular, I would like to express great thanks to Forrest Brinkley and Duane Marr for their patience and help.



TABLE of CONTENTS

ABSTRACT	ix
1. INTRODUCTION	1
2. INHERENT ERRORS IN CODE METHODOLOGY	6
3. MCNP COMPUTATIONAL STUDY AND RESULTS	12
4. THREEDANT COMPUTATIONAL RESULTS AND BENCHMARKING	25
5. FUTURE EXPERIMENTAL VERIFICATION	36
6. SUMMARY AND CONCLUSIONS	37
APPENDICES	
A: SAMPLE MCNP INPUT OUTPUT.....	58
B: SAMPLE THREEDANT INPUT/OUTPUT.....	61
REFERENCES	69

REACTIVITY EFFECTS OF VOID FORMATIONS IN A
SOLUTION CRITICAL ASSEMBLY

by

Steven G. Walters

ABSTRACT

SHEBA II (Solution High Energy Burst Assembly) was constructed in order to better understand the neutronics of solutions of fissile materials. In order to estimate the effect on criticality from the formation of bubbles, models were devised in MCNP (Monte Carlo Neutron Photon transport code) and THREEDANT (THREE dimensional, Diffusion-Accelerated, Neutral-Particle Transport). It was found that the formation of voids in all but the outside bottom edge of the assembly cylinder tend to act as a negative insertion of reactivity. Also, an experiment has been designed which will verify the results of the codes.

CHAPTER 1

INTRODUCTION

The purpose of this traineeship was to aid Los Alamos National Laboratory in understanding the characteristics of SHEBA II (Solution High-Energy Burst Assembly) as well as to benchmark the newly developed discrete-ordinates code THREEDANT (THREE dimensional, Diffusion-Accelerated, Neutral-Particle Transport). SHEBA II uses a low enriched (4.95%) uranyl fluoride solution (Anderson and Paternoster, 1984), and is intended for the evaluation of accidental criticality alarm detectors for enrichment plants, to benchmark calculations on a low-enrichment solution system, and to provide radiation fields to calibrate personnel dosimetry. An illustration of SHEBA II can be found following the text. When SHEBA II operates at its high-power level (two kilowatts), radiolytic gases should form at the rate of one liter per minute (Anderson and Paternoster). This bubble formation and its effect on reactivity is the focus of this paper.

Understanding the physics of a solution reactor is important because most spent fuels are stored as solutions. When nuclear fuel materials from power or production reactors are reprocessed, the reprocessing is invariably done by a chemical separation technique. The fuel, which is usually in oxide form (e.g., UO_2), is first dissolved with some type of acid (e.g., nitric, sulfuric, or hydrochloric acid). This turns the fuel into an aqueous solution. The presence of fissile isotopes and water in these solutions leads to concerns

regarding accidental criticalities with the solutions. When transported through pipes and stored in vessels, the possibility exists for the formation of bubbles. These bubbles could alter the geometric configuration of the fissile solution and in turn, affect the multiplicative state.

The construction of SHEBA II provides a means for studying the formation of voids in a fissile solution. The assembly vessel is a stainless steel cylindrical tank with a single safety rod along the axis which provides emergency shutdown capability without changing cylindrical symmetry. Control of the assembly is achieved by varying the solution level with a combination of pressure and vacuum through a single control handle. Rapid shutdown is accomplished by draining the solution through a three-inch valve. The critical assembly and the dump tanks are mounted on a pallet so that the distance above the ground may be varied. The important dimensions of SHEBA II that are used in the analysis are as follows.

Vessel diameter (inside)	=	48.26 cm
Vessel wall thickness	=	1.27 cm
Vessel height	=	121.92 cm
Central thimble diameter	=	6.35 cm
(outside)		
Central thimble thickness	=	0.635 cm
Gap between thimble and rod	=	0.3175 cm
Rod Cladding thickness	=	0.7937 cm

The primary tools used for this research were the computer codes MCNP (Monte Carlo Neutron Photon transport) and THREEDANT. MCNP was chosen because at the time the project began, no other code existed that could effectively perform eigenvalue calculations on non-symmetrical three-dimensional geometries. The theory of Monte Carlo is quite simple. One of the leaders in the theory was Stanislaw Ulam, who was working on a neutron diffusion problem at Los Alamos National Laboratory in the late nineteen forties. The problem considered a mass of uranium. The neutron moving through the mass collides with many atomic nuclei, and in each collision it can either elastically or inelastically scatter off the nucleus or else be absorbed by it. If the neutron is absorbed or inelastically scatters there is a chance that the nucleus will undergo fission and thereby introduce more neutrons to the problem. Ulam was trying to estimate how many neutrons would eventually escape from the lump and how many would remain behind to sustain a fission reaction. This problem was solved by playing the part of the neutron. Ulam would imagine moving through a lattice, occasionally colliding with atomic nuclei. At each collision he would randomly decide what would happen next, based on known probabilities. By following a neutron for hundreds of collisions, and then repeating the calculation for thousands of neutrons, he found that one can estimate important statistical properties of the neutron trajectories. Ulam eventually refined his theory and developed the current Monte Carlo theory with colleagues at Los Alamos (Carter and Cashwell, 1975).

Monte Carlo codes used to be the only codes capable of

efficiently numerically duplicating a statistical process in complex three-dimensional geometries. Monte Carlo methods are very different from deterministic transport methods. Deterministic methods, the most common of which is the discrete-ordinates method used by THREEDANT, solve the transport equation for the average particle behavior. By contrast, Monte Carlo methods do not solve an explicit equation, but instead the theory obtains answers by simulating individual particles, and recording certain aspects of their behavior. The average behavior of the particles in the physical system is inferred by the Central Limit theorem, from the average behavior of all the simulated particles. The main advantage of Monte Carlo is that non-symmetrical systems and very complicated geometries can be modeled. The main disadvantage of Monte Carlo theory is that a vast number of particles need to be generated in order to properly sample the problem.

The history of THREEDANT, the code that was used to check the results of MCNP, does not go back as far as MCNP. The original one-dimensional version of the code was developed between 1980-1982 by a group (T-1) at Los Alamos National Laboratory (Alcouffe, Brinkley, Marr, O'Dell, 1982). After the one-dimensional code (ONEDANT) came the two-dimensional version (TWOEDANT), which was just recently followed by the three-dimensional version. THREEDANT solves the multigroup transport equation in X-Y-Z or R--Z geometries (Clark, 1993). Many types of problems can be solved using THREEDANT, such as regular, adjoint, inhomogeneous or homogeneous (k_{eff} and eigenvalue search) problems. Also, these problems can be subject to

vacuum, reflective, periodic, white, or albedo boundary flux conditions. THREEDANT numerically solves the three-dimensional, multigroup form of the neutral-particle, steady-state form of the Boltzmann transport equation. The discrete-ordinates approximation is used for treating the angular variation of the particle distribution and the diamond-difference scheme is used for space discretization (Alcouffe, Brinkley, Marr, O'Dell, 1989). Negative fluxes are eliminated by a local set-to-zero and correct algorithm. A standard inner (within-group) iteration, outer (energy-group dependent source) iteration technique is used. Both inner and outer iterations are accelerated using the diffusion synthetic acceleration method. This acceleration method is what enables the code to converge in a manageable number of iterations.

CHAPTER 2

INHERENT ERRORS IN CODE METHODOLOGY

Although MCNP and THREEDANT may be considered the most advanced open codes to date of their respective types (Monte Carlo and discrete ordinates), one must keep in mind the inherent numerical errors that are associated with the codes. We will consider how errors are dealt with in MCNP first.

Monte Carlo results represent an average of the contributions from many histories sampled during the problem. While it is obvious that the results are important, the statistical error or uncertainty associated with the results cannot be overlooked. The importance of understanding the error cannot be overemphasized because of the insight that can be gained into the quality of the result. Monte Carlo results are obtained by sampling possible random walks and assigning a score x_i to each random walk. The scores assigned to each random walk will generally vary. We define a probability density function $p(x)$. By selecting a random walk, one adds x to the tally being estimated. The answer is the expected value of x , $E(x)$, where $E(x)$ is defined by the equation $E(x) = \int xp(x)dx = \text{true mean}$. $E(x)$ is seldom known because $p(x)$ is not known directly, but $E(x)$ can be estimated by Monte Carlo through the random walk process as , which is given by

$$= \frac{1}{N} \sum_{i=1}^N x_i \quad (1)$$

where x_i is the value of x selected from $p(x)$ for the i^{th}

history and N is the number of histories calculated in the problem. The Monte Carlo mean is the average value of the scores x_i for all the histories calculated in the problem. The relationship between $E(x)$ and σ^2 is given by the Strong Law of Large Numbers, which states that if $E(x)$ is finite, \bar{x} tends to the limit $E(x)$ as N approaches infinity (Briesmeister, 1986).

The variance of the population of x values is the measure of the spread in these values and is given by

$$\sigma^2 = \int (x - E(x))^2 p(x) dx = E(x^2) - (E(x))^2 \quad (2)$$

The square root of the variance is σ , which is called the standard deviation of the population of scores. As with $E(x)$, σ is seldom known but can be estimated by Monte Carlo for large N as S , given by the positive square root of

$$s^2 = \frac{\sum_{i=1}^N (x_i - \bar{x})^2}{N-1} \quad (3)$$

The quantity S is the estimated standard deviation of the population of x based on the value of \bar{x} that was actually sampled.

The estimated variance of \bar{x} is given by

$$(\sigma(\bar{x}))^2 = s^2 / N. \quad (4)$$

These equations do not depend on any restriction on the distribution of x or σ^2 beyond requiring that $E(x)$ and σ^2 exist and are finite. S is the standard deviation of the mean of \bar{x} , and it is important to note that S is proportional to $1 / \sqrt{N}$, which is

the inherent drawback to the Monte Carlo method. For instance, in order to reduce the quantity S by half, we must calculate four times the original number of histories.

Now that the concepts of the mean, variance, and the estimated standard deviation have been discussed with regard to MCNP, we introduce the inherent numerical errors associated with the methodology of THREEDANT. We cannot discuss the term standard deviation with regards to THREEDANT, because this applies to stochastic processes. The term does not apply to deterministic solutions such as discrete-ordinates codes. This is not to say that THREEDANT does not have inherent numerical errors. The numerical errors are due to, among other factors, how fine the meshes are in the input file. The meshes that can cause errors are the spatial mesh, the angular quadrature mesh, and the energy mesh that is built into the cross-section library. One way to minimize the errors associated with the meshes is to run a problem, try a finer mesh and see if the answer does not vary more than an acceptable criterion.

There is another error associated with the convergence process itself. The THREEDANT solver module employs the diffusion synthetic method to accelerate the iterative procedure used in solving the transport equation (Alcouffe, Brinkley, Marr, O'Dell, 1989). There are two different iterative procedures, one for problems containing fissionable material or energy-group upscattering and one for problems with neither fissions nor upscattering. The iterative strategy is divided into two parts, the inner iterations and outer iterations. The inner iterations are concerned with convergence of the pointwise

scalar fluxes in each group for a given source distribution. The outer iterations are concerned with the convergence of the eigenvalue, the fission source distribution and the energy-group upscatter source if any or all are present. The convergence of the iterations is monitored at both the inner and the outer iteration level. The inner iterations for a given energy are said to be converged when the pointwise scalar fluxes from one inner iteration to the next satisfy the condition (Alcouffe, Brinkley, Marr, O'Dell, 1989):

$$\max \left| (i,g^j - i,g^{j-1}) \right| < \text{epsi} \quad (5)$$

where i,g^j is the scalar flux for the mesh point i , group g , and inner iteration j , and epsi is the inner iteration convergence criterion set in the input file.

As the diffusion fluxes are calculated for each energy group, a new fission source rate distribution, $F(x)$ is calculated which is used to generate new diffusion fluxes. This process is repeated until both $F(x)$ and the pointwise fluxes are converged. The process of recalculation of $F(x)$ is called the diffusion sub-outer iteration. The convergence of the diffusion sub-outer iteration requires the satisfaction of two criteria. If we let n denote the outer iteration number and p denote the diffusion sub-outer iteration number, convergence of the diffusion sub-outer is then satisfied when both

$$\max \left| (i,g^p - i,g^{p-1}) / i,g^p \right| < 0.95*\text{epsx} \quad (6)$$

and

$$\left| 1 - D^{p'} \right| < \text{epso} \quad (7)$$

where

$$\text{epsx} \equiv \text{epsi} * [1 + \text{ngroup} * e^{(-100 * \text{epsi})}] \quad (8)$$

with ngroup being the number of energy groups.

The notation epso denotes the outer iteration convergence criterion, and

$$D^{p'} \equiv (F^{p'}, 1) / (F^{p-1}, 1) \quad (9)$$

with the notation (F,G) denoting the inner product (volume integral), of the product F*G.

Full convergence is achieved when the flux changes represented by Eqs. (5) and (6) are less than epsx with the additional requirements that (Alcouffe, Brinkley, Marr, O'Dell, 1989)

$$\max \left| (i, g^1 - i, g^0) / i, g^0 \right| < \text{epsx} \quad (10)$$

and

$$\left| 1 - \right| < \text{epso}, \quad (11)$$

where i, g^1 , represents the scalar flux at point i, group g from the first diffusion sub-outer iteration for outer iteration and i, g^0 , denotes the scalar flux at point i, group g from the last diffusion inner iteration of outer iteration .

The evaluation of the error in the result of THREEDANT is

not as straight forward as with MCNP. The rule of thumb is that the answer is within $3 \cdot \text{eps}$, where eps is the convergence criteria. This rule of thumb is for well behaved convergence. That is, if the problem converges in only ten or twenty iterations, then there is a good assurance that the problem is well behaved¹ as long as the global balance is less than roughly $1.0e-6$ for eigenvalue problems.

¹ In past discrete-ordinates codes, certain problems were very slow to converge. One such problem was one with a lot of upscatter in the cross-section set. These problems might change very little with outer iteration even though the k effective was still far from the converged value. But the code would have satisfied the convergence criterion that was in the input file, and one might think the final answer was at hand. Typically, these runs might take over 40 iterations. With the acceleration techniques used in THREEDANT, one does not experience these sorts of problems.

CHAPTER 3

MCNP COMPUTATIONAL STUDY AND RESULTS

MCNP was used to calculate the reactivity effects of the formation of radiolytic bubbles in SHEBA II. These bubbles were modeled as a very low density nitrogen (10^{-9} g/cm³) in MCNP, because making a particular cell a void in the MCNP input file would result in no tallies being collected in that particular cell. The first summer² was spent at Los Alamos National Laboratory as an introduction to the theory of MCNP, its input structure, as well as a period of acclimation to the laboratory and its computer systems. The second summer was when most of the research for the project was conducted. The computational study of SHEBA II was conducted on a variety of machines. During the first summer, the computer modeling was performed mainly on a CRAY at Los Alamos. During the second summer, the computer modeling was conducted on a variety of machines that included a SPARC I, SPARC II, SPARC 10, and a DEC 5000 at North Carolina State University.

The modeling in MCNP considered four different void positions (low density nitrogen bubble), all with the same volume (581 cm³). This volume was selected after a sensitivity study was performed which demonstrated that a volume of this magnitude was needed to overcome the statistical error inherent to Monte Carlo methods. The solution height in the input file

² A typical fifteen month M.N.E. program involves the initial two months of the program being spent performing preliminary research into the project. These two months are followed by two semesters of course work and then the final four months of research.

was set to take into account the displacement of the solution from the void (i.e., maintaining constant fluid volume). This displacement was consistent between both MCNP and THREEDANT and increased the initial voided solution height by 0.323397 centimeters. The void was modeled as a cylindrical annular segment Fig. 19. This configuration was chosen to maintain consistency between the geometric models of MCNP and THREEDANT³. The first position considered was the outside bottom of the cylinder. This position was selected for two reasons. First, this position will be the same as if the void was placed at the top of the solution along the edge of the cylinder, due to the effects of symmetry. Furthermore, of all the positions, this one originally was considered intuitively as the one with the greatest chance of acting as a positive insertion. The next position considered was at the midplane of the solution along the outside of the cylinder. The final two positions are at the same vertical positions as the other two voids, but they exist along the central thimble, slightly off the central axis of the cylinder.

The modeling was performed by creating an input file in the format of MCNP. The input file modeled SHEBA II and its immediate surroundings to a high amount of detail. An example input file for MCNP can be found in Appendix A. Because SHEBA II has only slightly different dimensions than SHEBA (a predecessor to SHEBA II) and the uranyl fluoride solution is the same, the approximate critical height was known. A height for

³ MCNP is able to handle different coordinate systems in the same input file. This feature is quite different from THREEDANT, which is unable to mix coordinate systems .

the solution was selected initially that was within a few centimeters of the critical height of SHEBA.

During the first summer, a technique was acquired which lowered the estimated standard deviation of the selected output tallies from MCNP. This technique involved performing a pre-production run of approximately 80 cycles of each different void position. A source distribution file is created by MCNP, which is used in a production run to lower the estimated standard deviation. If a source distribution file was not used, the large estimated standard deviation from the first dozen cycles would be averaged into the final estimated standard deviation and thus increase the size of the final deviation. The production run was for 350 cycles. While this large number of cycles was computer and time intensive, a smaller number would produce a larger estimated standard deviation, but a larger number of cycles would not improve the statistics significantly since the estimated standard deviation is proportional to $1 / \sqrt{N}$, where N is the number of histories. A graph of the $1 / \sqrt{N}$ behavior of the estimated standard deviation can be found in Fig. 1.

Before any runs were conducted that contained voids, the critical height without any voids needed to be determined with MCNP. The input file was constructed and run, and the results were then examined. To verify that the input file was modeling the problem that was intended, the output was analyzed. For example, small cells were placed every 0.5 centimeter at the midplane of the cylinder from the central thimble to the outside of the cylinder in order to plot the neutron flux profile. This

plot can be seen in Fig. 2. As can be seen, the flux profile is acting as one would expect with the highest flux being towards the center of the cylinder while it decreases as it goes out radially from the center of the cylinder, in a $J_0(r)$ -like behavior.

Once it was fairly certain that the input file was modeling the problem accurately, the critical height with no voids in the model needed to be determined. Nine different heights were run and their associated k_{eff} were plotted versus the solution heights. The results of the runs can be seen in Table 1 below and the corresponding graph can be found in Fig. 3. As can be seen from Fig. 3, the approximate critical height is 41.31 ± 0.29 centimeters, where the deviation of the height is found from the linear fit of the line. The standard deviation of the height for two particular points was obtained by using the following procedure. By selecting two points on Fig. 3 such as the solution heights of 40.00 and 41.00 centimeters and their respective k_{eff} values of 0.99535 and 0.99874, the reactivity per centimeter (ρ 0.5215) can be calculated. With the reactivity per centimeter and the reactivity of the estimated standard deviation (ρ 0.1654), which is found in the output file, the estimated deviation of the height is obtained. For example using the for thermal U^{235} fissions (0.0065), the standard deviation of the height is found.

$$0.99874 - 0.99535 = 0.00339 \text{ per centimeter}$$

$$0.00339 / 0.0065 = \$0.5215 \text{ per centimeter}$$

$$0.0011 / 0.0065 = \$0.1654$$

standard deviation of height =

$$\$0.1654 / \$0.5215 \text{ per cm} = 0.3171 \text{ cm}$$

TABLE 1

Solution heights and k_{eff}

(MCNP: no void in cylinder)

Solution Height (cm)	k_{eff}	Estimated Relative Standard Deviation (\pm)
39.50	0.991442	0.0010
40.00	0.995347	0.0012
40.50	0.996716	0.0009
41.00	0.998737	0.0010
41.25	0.999983	0.0010
41.50	1.000950	0.0010
42.00	1.003220	0.0009
42.50	1.005190	0.0010

The first void position that was analyzed was with the void at the outside bottom of the cylinder. A new input file was created with everything identical to the original input file

(no-void) except that a cell that represented a void was placed at the outside bottom of the cylinder. With the approximate critical height being known from the no-void case, a solution height was selected that was a few centimeters below critical height. The case was run and a new input file was created with a slightly higher solution height (0.25 cm). This cycle would continue until the solution height was a few centimeters above critical height. A comparison of k_{eff} versus the solution height can be found in Table 2. The graph of the data can be seen in Fig. 4.

TABLE 2

Solution and k_{eff}

(MCNP: void placed at outside bottom of cylinder)

Solution Height (cm)	k_{eff}	Estimated Relative Standard Deviation (\pm)
41.216	0.99669	0.00109
41.466	0.99782	0.00107
41.716	0.99976	0.00114
41.966	0.99978	0.00108
42.216	1.00019	0.00109
42.466	1.00193	0.00105
42.716	1.00296	0.00077
42.966	1.00325	0.00113

The next void position that was modeled was with the void at the outside midplane of the cylinder. A new input file was created with everything identical to the last input file (void at outside bottom) except for the void position. Following the same procedure as before, multiple cases were run. The solution height varied from 41.2 to 43.2 centimeters. A table of k_{eff} versus the solution height can be found in Table 3, and a graph of the data can be found in Fig. 5.

TABLE 3

Solution heights and k_{eff}

(MCNP: void placed at outside midplane of cylinder)

Solution Height (cm)	k_{eff}	Estimated Relative Standard Deviation (\pm)
41.216	0.99256	0.00109
41.466	0.99364	0.00116
41.716	0.99669	0.00113
41.966	0.99699	0.00108
42.216	0.99824	0.00111
42.466	0.99972	0.00106
42.716	1.00032	0.00102
42.966	1.00119	0.00109
43.216	1.00313	0.00109

The next void position that was modeled was with the void at the inside midplane of the cylinder. Following the same procedure as before, multiple cases were run. A table of the k_{eff} versus the solution height can be found in Table 4, and a graph of the data can be found in Fig. 6.

TABLE 4

Solution heights and k_{eff}

(MCNP: void placed at inside midplane of cylinder)

Solution Height (cm)	k_{eff}	Estimated Relative Standard Deviation (\pm)
41.466	0.99315	0.00122
41.716	0.99489	0.00116
41.966	0.99643	0.00132
42.216	0.99668	0.00129
42.466	0.99820	0.00111
42.716	0.99972	0.00106
42.966	1.00066	0.00102
43.216	1.00100	0.00122
43.466	1.00209	0.00134
43.716	1.00237	0.00111
43.966	1.00356	0.00106

The final void position that was modeled was with the void at the inside bottom of the cylinder. A new input file was created with everything identical to the last input file except for the void position. Following the same procedure as before, multiple cases were run. A table of k_{eff} versus the solution

height can be found in Table 5, and a graph of the data can be found in Fig. 7.

TABLE 5
 Solution heights and k_{eff}
 (MCNP: void placed at inside bottom of cylinder)

Solution Height (cm)	k_{eff}	Estimated Relative Standard Deviation (±)
41.466	0.99474	0.00117
41.716	0.99631	0.00123
41.966	0.99723	0.00126
42.216	0.99818	0.00114
42.466	0.99810	0.00126
42.716	1.00014	0.00106
42.966	1.00084	0.00124
43.216	1.00384	0.00127
43.466	1.00707	0.00134
43.716	1.00947	0.00111

The running of all void positions as well as the no-void case took approximately 550 CPU hours, or 23 days of constant CPU usage on a SPARC I. It must be noted that all void positions cannot be compared to each other. The voids placed at

the outside of the cylinder can be compared because these voids have the same dimensions, but are at different positions in the tank. The same argument can be made for the voids that are at the inside of the tank adjacent to the central thimble. The difference in void dimensions makes the comparison of the inside position and outside position impossible even though these voids have the same volume. But from MCNP results, it can be said that all voids act as a negative reactivity insertion when compared to the no-void case (Fig. 8).

The fact that the void at the outside of the cylinder has a negative worth, as seen in Fig. 9, is not surprising when one considers the physics of the matter. It is known that a void placed at the outside edge of the cylinder will increase leakage, lower the number of fission events, and hence lower the k_{eff} . It would seem apparent that the void positioned at the outside bottom of the cylinder would have a more negative worth when compared to the void at the outside midplane of the cylinder if one just considered the surface area of leakage. But the void positioned at the outside midplane of the cylinder encounters more neutrons due to its greater solid angle than the void positioned at the outside bottom. Another way of looking at why the void at the outside bottom of the cylinder does not have as negative a worth is to consider the importance of the different regions with respect to the neutrons. The region at the outside bottom of the cylinder does not encounter as many neutrons as the void at the midplane of the cylinder. This region can be considered to have a lower importance with respect to neutrons. When this region is replaced by a void, there is

increased leakage in the area which will act as a negative insertion. But this void displaces the top of the solution 0.323397 centimeters up. The solution that was in the volume that the void now occupies is spread out evenly over the top of the solution. While it is true that some of the solution is toward the outside of the cylinder, some is also in the center of the cylinder which has a higher importance. This displacement of solution around the central thimble acts as a slight positive insertion. This slight insertion offsets some of the negative insertion that is obtained from the leakage at the bottom of the cylinder.

If a void formation toward the center of the tank is considered (around the central thimble) it can be seen in Fig. 10 that both positions (midplane and bottom) act as a negative reactivity insertion. The reasons for the negative worths are different depending on the location of the void. For instance, if the void forms on the bottom of the tank around the central thimble there is a large increase in leakage due to the void. The void causes an increase in leakage because neutrons that would normally be in fissionable material, if the void was not there, are able to pass through the void and out of the system. This loss of neutrons reduces the number for fission, and hence decreases k_{eff} .

If one considers the formation of a void around the central thimble at the midplane of the solution height, it also acts as a negative insertion, but for different reasons. When a void is modeled around the central thimble, it displaces a large volume of fissionable material from an area of high importance

to one of low importance. This displacement of material is enough to account for the negative worth of the void, even though there is not any leakage.

CHAPTER 4

THREEDANT COMPUTATIONAL RESULTS AND BENCHMARKING

With the results from MCNP in hand, an experiment was designed in the second summer of my M.N.E (Master of Nuclear Engineering) traineeship that would have verified the results obtained through MCNP. Unfortunately, bureaucratic complications arose which made the experiment impossible to run in the time frame of my project. While this experiment will hopefully be performed sometime in the future, it was decided to verify the results of MCNP computationally. With the existence of a new code capable of modeling non-symmetrical geometries and a need for this code to be benchmarked, it was decided that this code would be used in place of the experiment to verify MCNP.

An input file for THREEDANT was created in order to obtain the k_{eff} of SHEBA II without the existence of voids. For all the THREEDANT runs, the angular quadrature order is eight, the number of mesh points are roughly 25,000, and the sixteen group cross-section set is ENDFB-V. The input files were run until the k_{eff} eigenvalue had converged to 1×10^{-4} . Even with this liberal convergence limit, at times the code did not converge to all criteria. When this happened it was effectively ignored and the last iteration number was used if there was convergence to at least four significant figures. Numbers were taken to six significant figures after the decimal, but only the first four are reliable. A sample input file for THREEDANT can be found in Appendix B. Similar to the procedure used in MCNP, various solution heights were run and the data can be found in the Table

6. The corresponding graph can be found in Fig 11.

TABLE 6

Solution heights and k_{eff}

(THREEDANT: no void in cylinder)

Solution Height (cm)	k_{eff}	Estimated Error (±)
41.46	0.988542	0.0003
42.46	0.993191	0.0003
43.00	0.995392	0.0003
43.50	0.997492	0.0003
44.00	0.999543	0.0003
44.50	1.001534	0.0003
45.00	1.003325	0.0003
45.46	1.005314	0.0003

As with MCNP, the first void position that was analyzed in THREEDANT was with the void at the outside bottom of the cylinder. A new input file was created with most things identical to the original input file (no void) except that a cell was set up at the outside bottom of the cylinder that represented a void. The void representation also changed the spatial mesh from the last case. A number of test cases were submitted where the spatial mesh was varied until there was no

significant change in the results. This procedure lead to confidence in the spatial mesh that was used in the problem. This procedure of varying the spatial mash in order to find a suitable mesh was used in all the different void positions. With the approximate critical height being known from the no-void case, a solution height was selected that was a few centimeters below critical height. The same procedure used in MCNP to obtain the critical height was used here. Different cases were run with the solution height varying. The outputs were analyzed, and the k_{eff} for each solution height was noted. A comparison of k_{eff} versus the solution height can be found in Table 7, and a graph of this data can be found in Fig. 12.

TABLE 7

Solution and k_{eff}

(THREEDANT: void placed at outside bottom of cylinder)

Solution Height (cm)	k_{eff}	Estimated Error (\pm)
41.96	0.988806	0.0003
42.46	0.992652	0.0003
42.72	0.993747	0.0003
42.96	0.994827	0.0003
43.22	0.995891	0.0003
43.46	0.997137	0.0003
43.72	0.998041	0.0003
43.96	0.999019	0.0003
44.46	1.001020	0.0003
44.96	1.002970	0.0003
45.46	1.004300	0.0003

The next void position that was modeled was with the void at the outside midplane of the cylinder. A new input file was created with everything identical to the last input file (void at outside bottom) except for the void position. Following the same procedure as before, multiple cases were run. The solution height was varied and a table of the k_{eff} versus the solution height can be found in Table 8. A graph of the data can be found in Fig. 13.

TABLE 8

Solution heights and k_{eff}

(THREEDANT: void placed at outside midplane of cylinder)

Solution Height (cm)	k_{eff}	Estimated Error (\pm)
41.96	0.987322	0.0003
42.46	0.989565	0.0003
42.96	0.991744	0.0003
43.46	0.993885	0.0003
43.96	0.995961	0.0003
44.46	0.998325	0.0003
44.96	1.000590	0.0003
45.46	1.002740	0.0003
45.96	1.004710	0.0003
46.96	1.006690	0.0003

A void at the inside midplane of the cylinder was modeled next. A new input file was created with the void position changed. Again, cases were run with varying solution heights. A table of the k_{eff} versus the solution height can be found in Table 9, and a graph of the data can be found in Fig. 14.

TABLE 9

Solution heights and k_{eff}

(THREEDANT: void placed at inside midplane)

Solution Height (cm)	k_{eff}	Estimated Error (\pm)
41.96	0.987420	0.0003
42.46	0.989865	0.0003
42.96	0.992044	0.0003
43.46	0.994192	0.0003
43.96	0.996261	0.0003
44.46	0.998625	0.0003
44.96	1.000620	0.0003
45.46	1.003040	0.0003
45.96	1.004820	0.0003
46.46	1.006990	0.0003

Finally, a void was modeled at the inside bottom of the cylinder. Following the same procedure as before, multiple cases were run of this new input file. The solution height varied from 42.46 centimeters to 46.96 centimeters. Table 10 contains a comparison of k_{eff} versus the solution height. A graph of the data can be found in Fig. 15.

TABLE 10

Solution and k_{eff}

(THREEDANT: void placed at inside bottom of cylinder)

Solution Height (cm)	k_{eff}	Estimated Error (\pm)
41.46	0.985762	0.0003
41.96	0.988098	0.0003
42.46	0.990384	0.0003
42.96	0.992586	0.0003
43.46	0.994760	0.0003
43.96	0.996853	0.0003
44.46	0.998898	0.0003
44.96	1.001004	0.0003
45.46	1.003110	0.0003
45.96	1.005853	0.0003

As with the run time per case in MCNP, each case in THREEDANT took approximately 12-25 hours depending on the computer used. Also as with the CPU time of MCNP, the total run time of THREEDANT was approximately 500 CPU hours on a SPARC I. It can be seen in Fig. 16 that all the void positions, except the void at the outside bottom of the cylinder, act as a negative worth. The void at the outside bottom of the cylinder has a slightly positive worth, as seen in Fig. 17, when one considers that the void automatically displaces the top of the

solution 0.323397 centimeters. The possibility of a positive insertion by this void was originally considered and is not startling when one considers that this position has a low importance, thus leakage is not severe. Also, fissile solution is being displaced from a region of low importance to a region of higher importance (on average), which would increase fissions and hence k_{eff} . While these results are different from MCNP, the trends (i.e., the voids worth relative to each other) that result from THREEDANT agree quite well with the results of MCNP. Also, as can be seen in figures 3-7 and 11-15, the slopes of all of these figures are similar. This fact provides a useful calculational benchmark for THREEDANT because the relatively consistent slopes lead to the calculation of roughly the same amount of reactivity per centimeter, regardless of which code is considered.

As can be seen in Fig. 18, the results from THREEDANT show that the formation of voids toward the inside of the cylinder (around the central thimble) act as a negative reactivity insertion as in MCNP. The reason for this negative worth is dependent on position. For instance, a void at the inside bottom of the cylinder promotes leakage while a void at the inside midplane displaces solution from an extremely important region to one of relatively low importance.

A comparison of the critical heights of all void positions calculated in THREEDANT and MCNP can be found in Table 11. If we take into account that the displacement of the void automatically raises the solution height 0.323397 cm, the change in height required to make the system critical can be

found in Table 12. As can be seen in the tables, for all the void cases there is roughly a two centimeter difference between the critical height in MCNP and THREEDANT for all void positions.

TABLE 11

Comparison of the critical heights

Void Position	MCNP	THREEDANT
No Void	41.31 ± 0.29 cm	44.13 cm
Outside bottom	42.13 ± 0.33 cm	44.26 cm
Outside midplane	42.61 ± 0.26 cm	44.62 cm
Inside bottom	42.64 ± 0.21 cm	44.78 cm
Inside midplane	42.71 ± 0.33 cm	44.72 cm

TABLE 12

Comparison of the change in heights to
maintain criticality with the void displacement
taken into account

Void Position	MCNP	THREEDANT
No Void	41.31 ± 0.29 cm	44.13 cm
Outside bottom	+ 0.50 ± 0.33 cm	- 0.19 cm
Outside midplane	+ 0.98 ± 0.26 cm	+ 0.17 cm
Inside bottom	+ 1.01 ± 0.21 cm	+ 0.33 cm
Inside midplane	+ 1.08 ± 0.33 cm	+ 0.27 cm

As to why there is the two centimeter difference remains to be seen. In 1991, an analysis of rod worths in SHEBA II was performed (Kornreich). It was discovered that TWODANT consistently gave a higher critical height (~ 2cm) than MCNP. Further analysis was performed which involved obtaining the critical height of SHEBA (which was known from experiment), with MCNP and TWODANT. TWODANT, using the same cross-section set as was used in this analysis, gave a more accurate answer than MCNP

as can be seen in Table 13.

TABLE 13

Comparison of the critical heights

	Experiment	MCNP	TWODANT
SHEBA	36.5 cm	34.9 cm	36.6 cm
SHEBA II	?	41.3 cm	44.1 cm

While no reason was given at the time for the critical height differences, it has been suspected that the problem existed in the cross-section set that was used. MCNP was used with a continuous energy cross-section set, while THREEDANT was used with a sixteen-group set. The continuous energy set has an apparent advantage in that it treats the energy range not as groups but as a continuous energy range, where the sixteen group set breaks the energy range into sixteen distinct groups. But, the cross-section set used in THREEDANT was constructed by Hansen and Roach. The strength of this set is that it treats the resolved and unresolved resonances and has been in use for decades with a high amount of success (i.e., has been benchmarked against many critical assemblies). As far as the benchmarking of THREEDANT goes, it is very encouraging that the trends that existed in the MCNP runs also exist in the THREEDANT results.

CHAPTER 5

FUTURE EXPERIMENTAL VERIFICATION

As was mentioned in Chapter 4, an experiment has been designed that will be used to test the accuracy of the codes. The experiment is designed to simulate the formation of voids in the reactor cylinder of SHEBA II. The voids are to be made of aluminum, which was selected due to its relatively small cross section to neutrons as well as its ability to form a protective oxide layer. Although this layer would ultimately be destroyed by the corrosive properties ($\text{pH} = 1$) of the uranyl fluoride solution, it would provide adequate protection for the time frame of the experiment. The details of the void design can be found in Fig. 19. A mechanism was also designed which would place the voids into the different positions. Although at this time the voids and support mechanism have not been fabricated, it is hoped that they will be done prior to the first approach to critical of SHEBA II. One point of safety should be noted. Because the void at the outside midplane of the cylinder has a more negative worth than a void placed below it at the outside bottom of the cylinder, care should be taken to insure that it does not fall after going critical with it in position. If a void at the outside midplane of the cylinder were to fall unexpectedly, this change in position would act as a positive insertion of roughly between $\$0.19$ and $\$0.40$.

CHAPTER 6

SUMMARY AND CONCLUSIONS

The effect of a void formation in a solution critical assembly has been found. The modeling of these voids has been performed in two codes. The first, MCNP (Monte Carlo Neutron Photon transport), is a Monte Carlo code. The second, THREEDANT (THREE dimensional, Diffusion-Accelerated, Neutral-Particle Transport), is a discrete-ordinates code. Four voids were modeled in four distinct positions. It is apparent that the formation of a void in all but the outside bottom of the cylinder acts as a negative reactivity insertion. It also is evident that a void placed at the outside bottom of the cylinder does not have as negative a worth as a void placed at the other positions in the cylinder, or possibly even has a slightly positive worth. The reason for the less negative worth for a void placed at the outside bottom of the cylinder is due to competing effects. For instance, while it is true that a void in this position is increasing leakage, it is also displacing fissionable material to a region that is considered more important to neutron interaction.

An experiment has been devised which will be able to verify the results of the codes. This experiment will hopefully be performed in the near future, and consists of inserting aluminum voids in the shape that was used in the codes. A mechanical device was also designed which would be able to insert the voids in various positions.

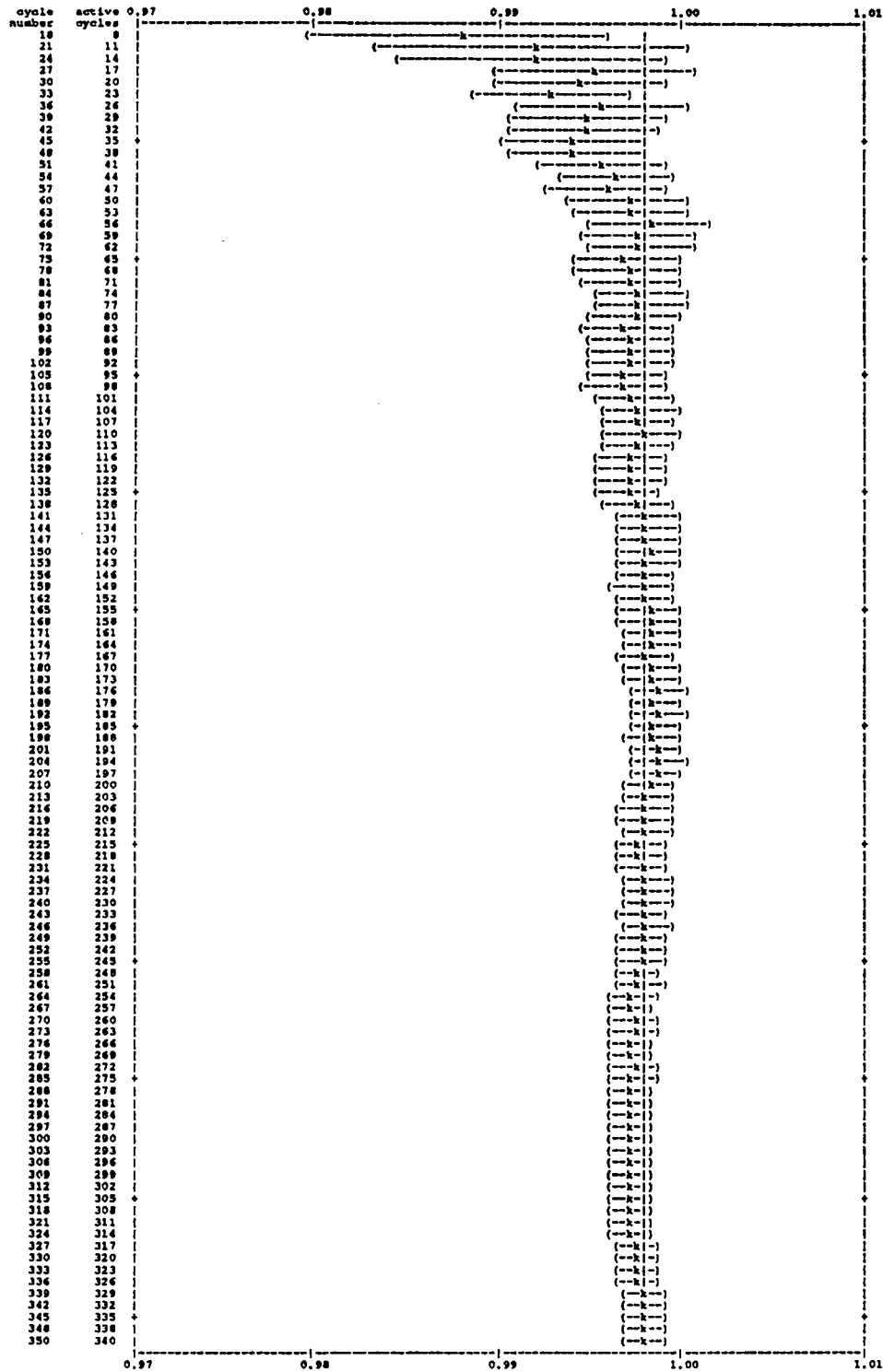
Finally, THREEDANT was used not only to verify

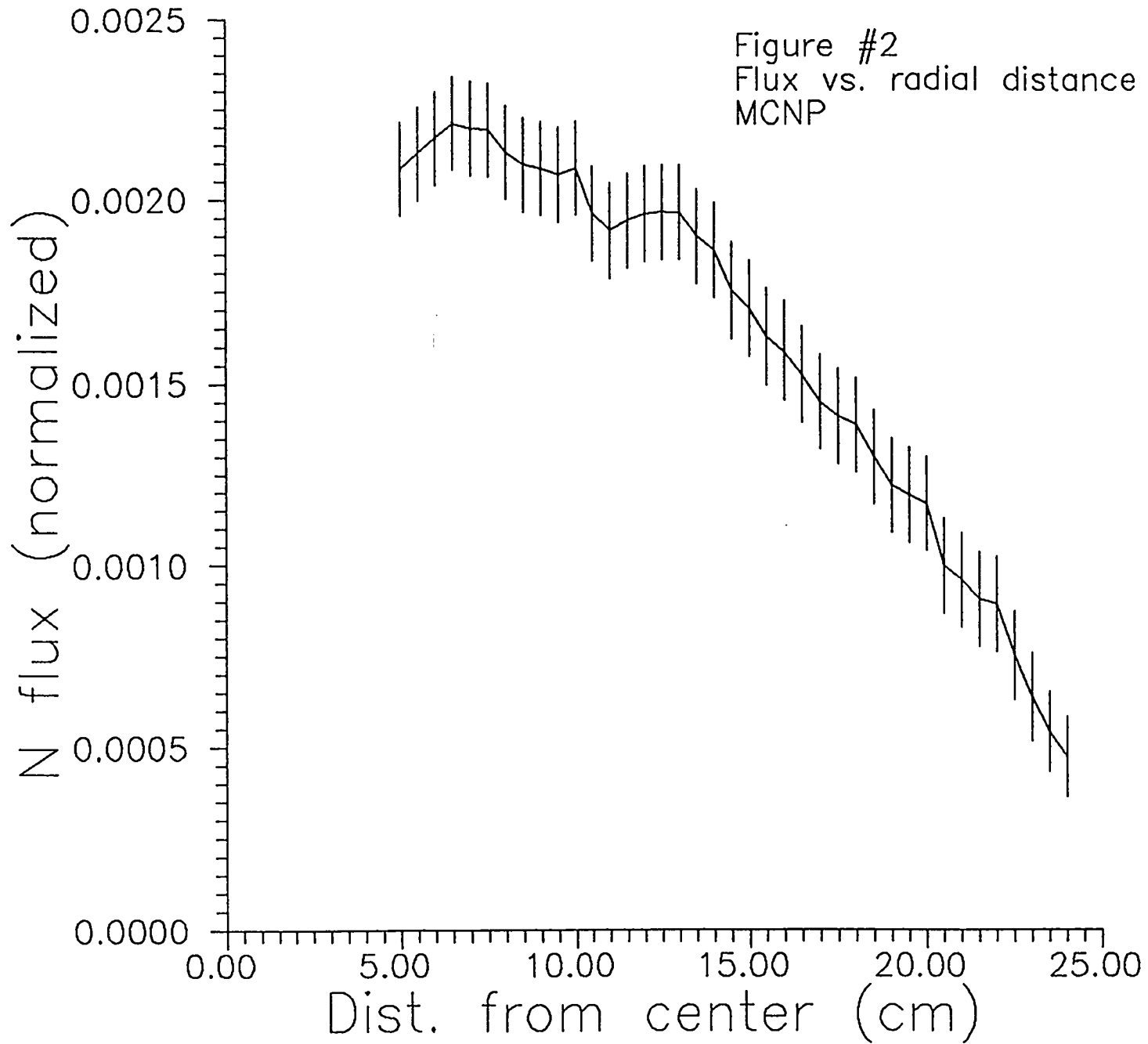
MCNP, but the need existed for the benchmarking of this new code. It was quite encouraging to see that both codes (MCNP and THREEDANT) gave results that have the same trend. Both codes resulted in roughly the same slopes when the k_{eff} versus solution height was plotted. This roughly consistent slope led to the calculation of similar worths per centimeter of the solution. Although the slopes were similar between the two codes, the critical heights were not. When voids were modeled in various positions, approximately two centimeters separated the critical heights given by MCNP and THREEDANT. A consistent discrepancy, as in this case, suggests that the discrepancy could be the result of differences in the cross-section sets. While the cross-section differences are a possible solution, future analysis will need to be conducted in order to have increased confidence in this solution. In conclusion, it seems that employing both neutronics codes has provided insight into the codes and their capabilities, as well as to the effects of the voids on reactivity.

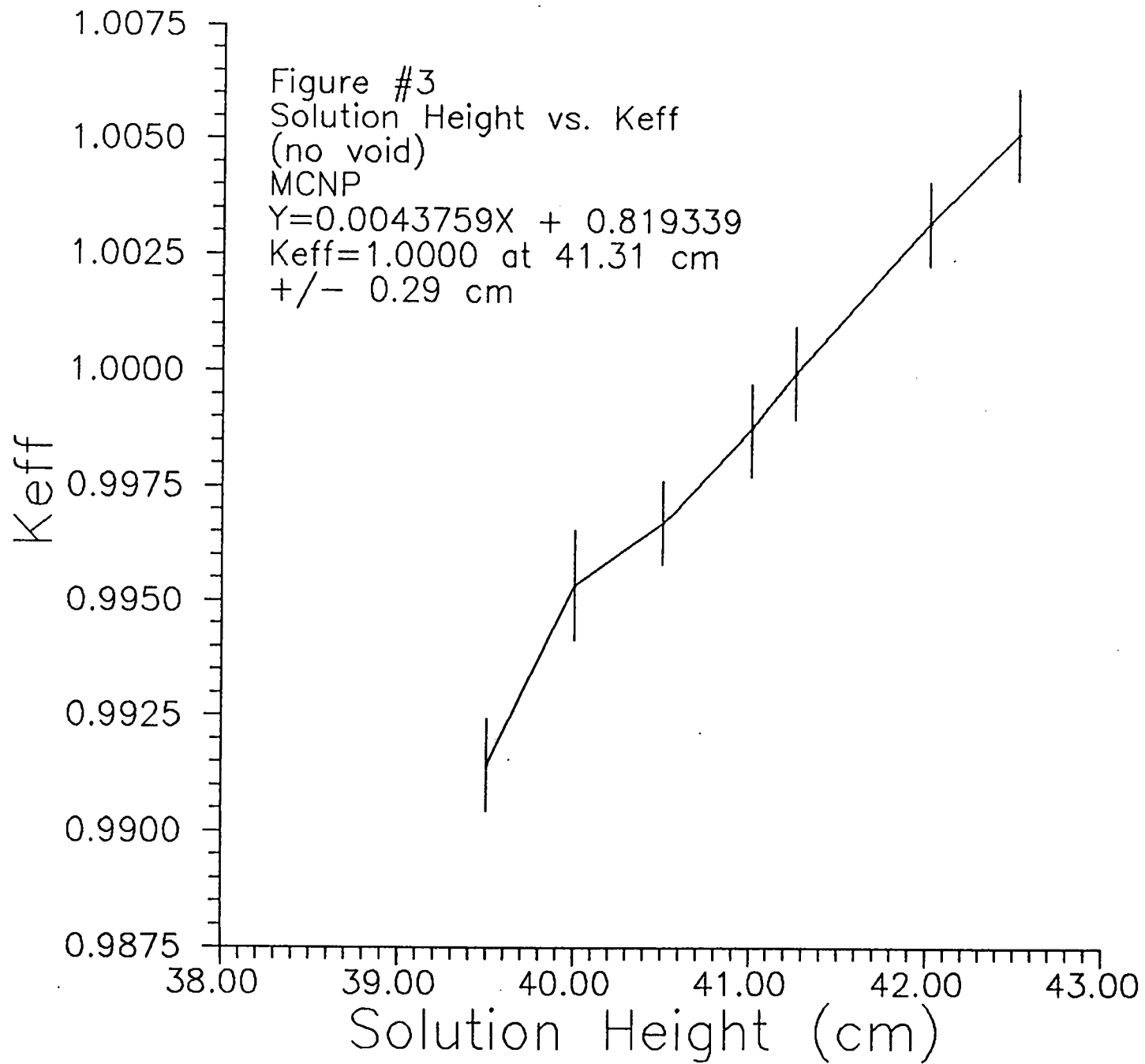
Figure #1

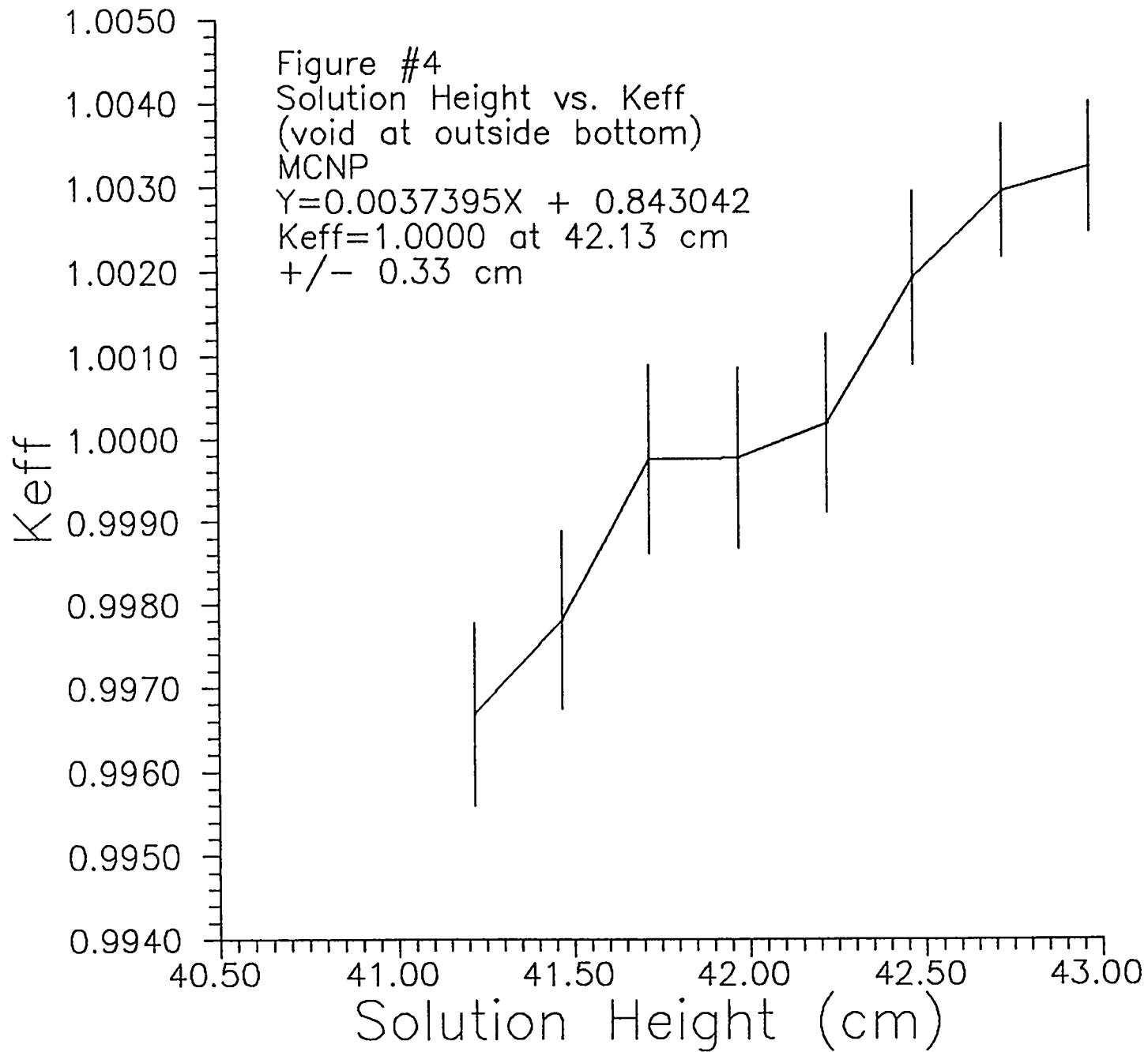
(1 / \sqrt{N} characteristic of estimated standard deviation)

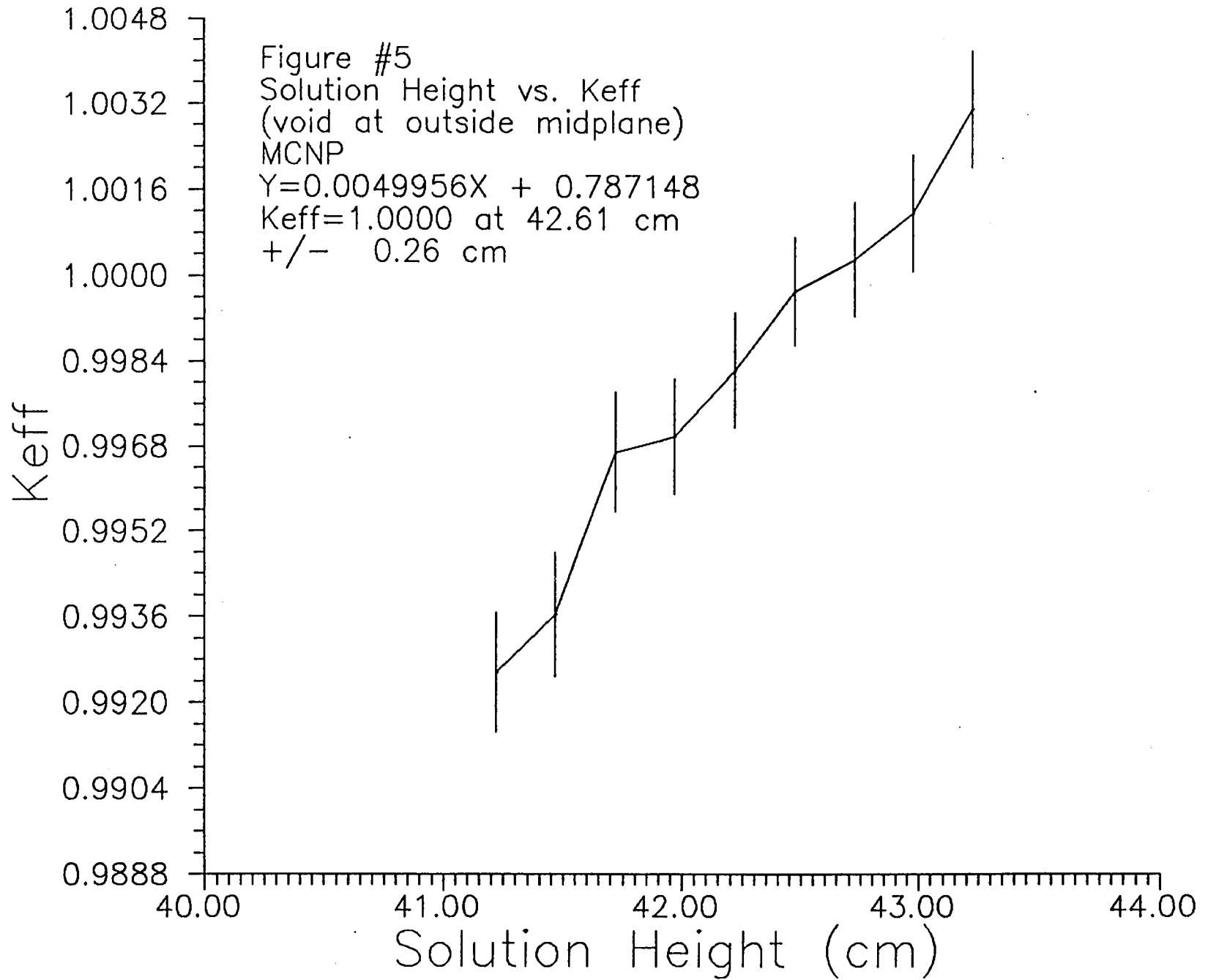
plot of the estimated oel/abs/track-length heff one standard deviation interval versus cycle number (l = final heff = 0.99803)

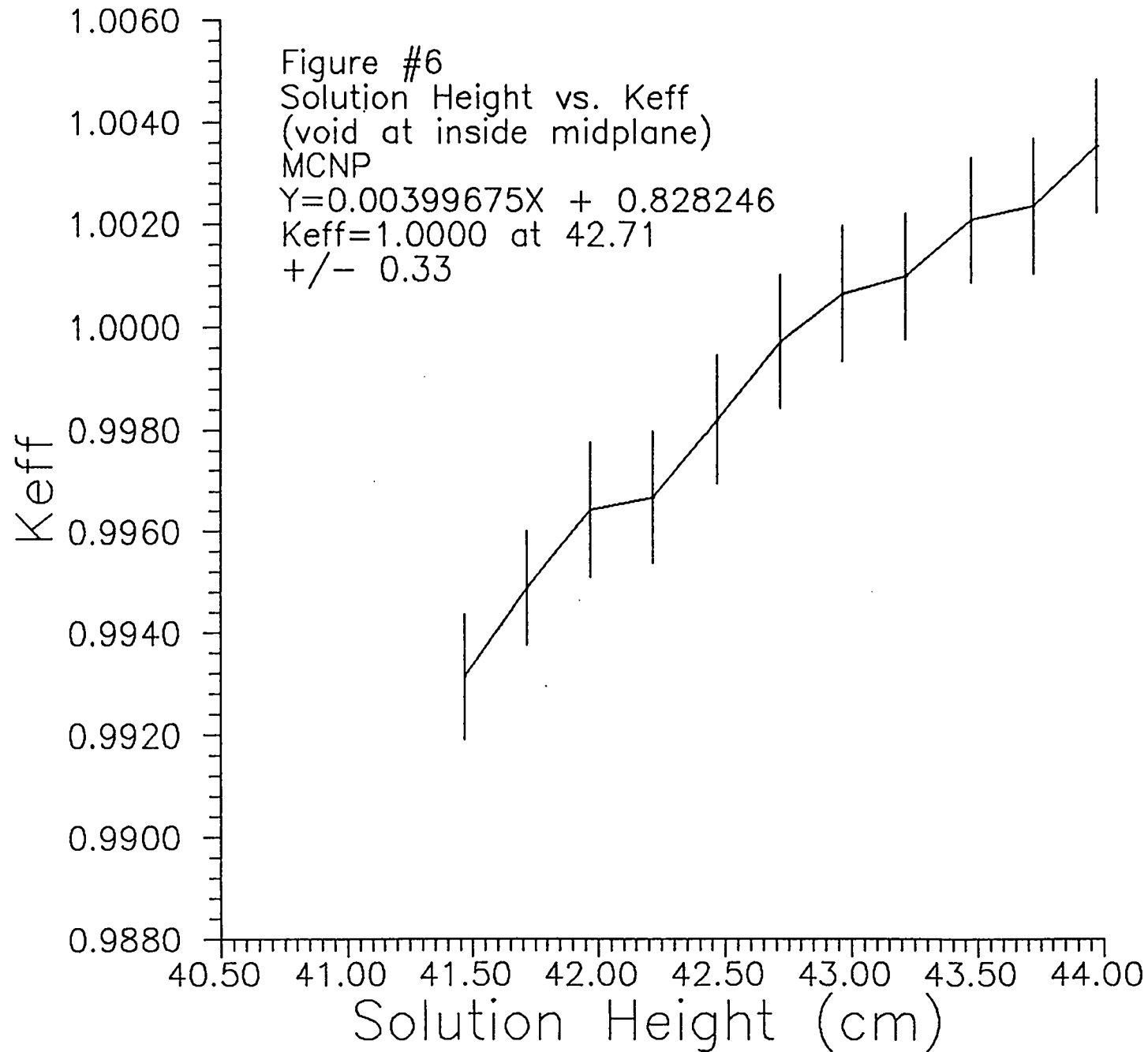


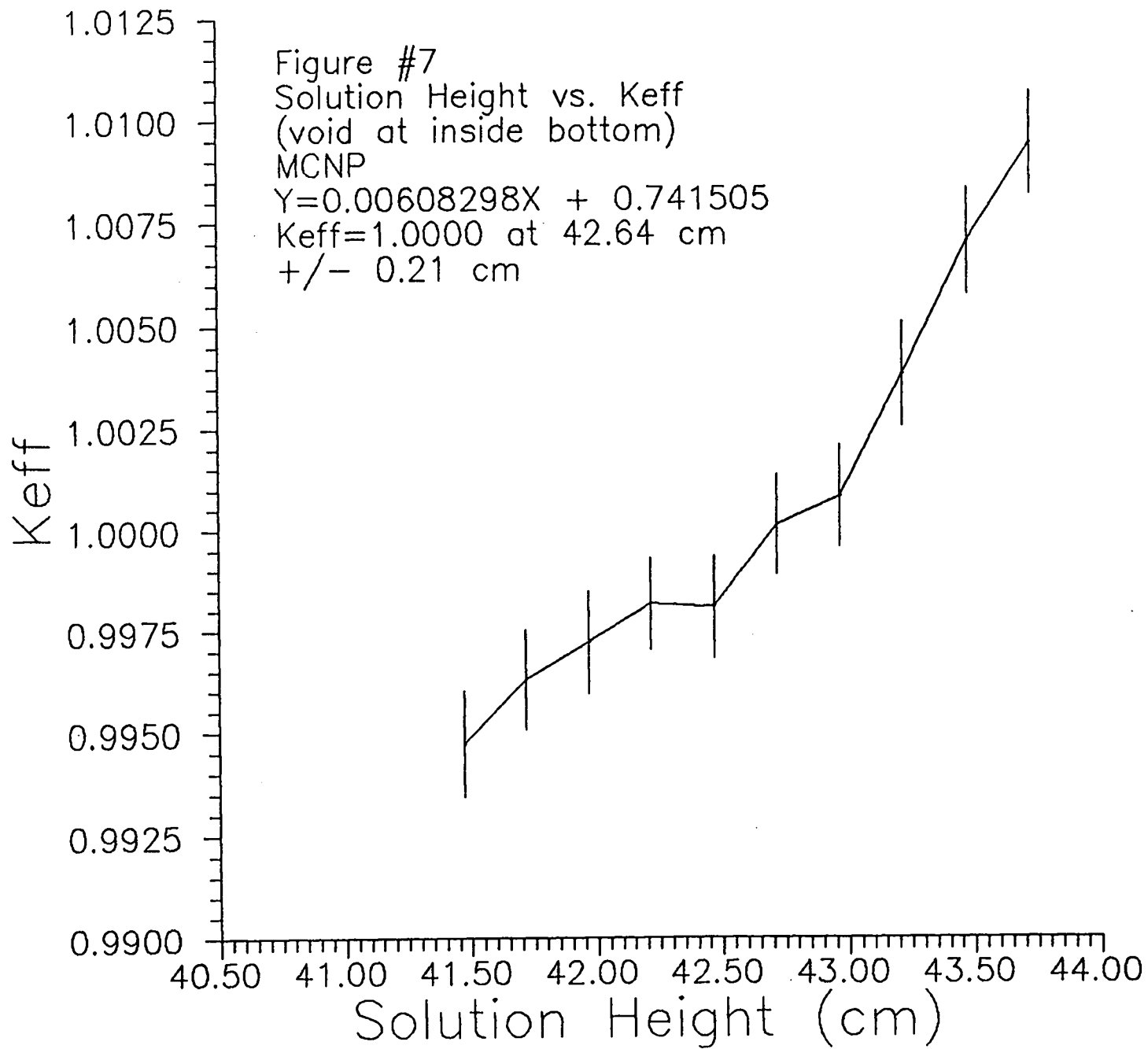


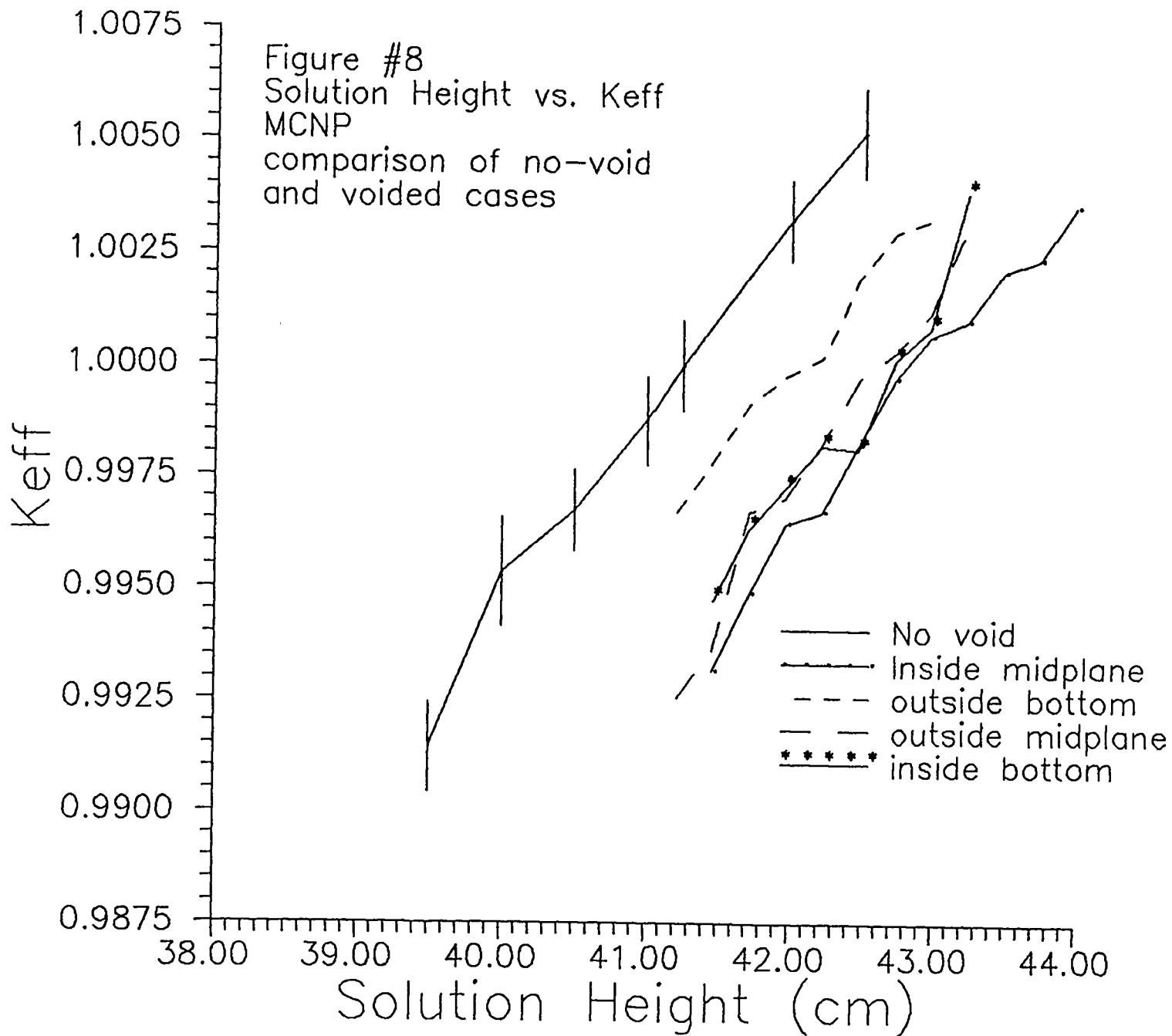


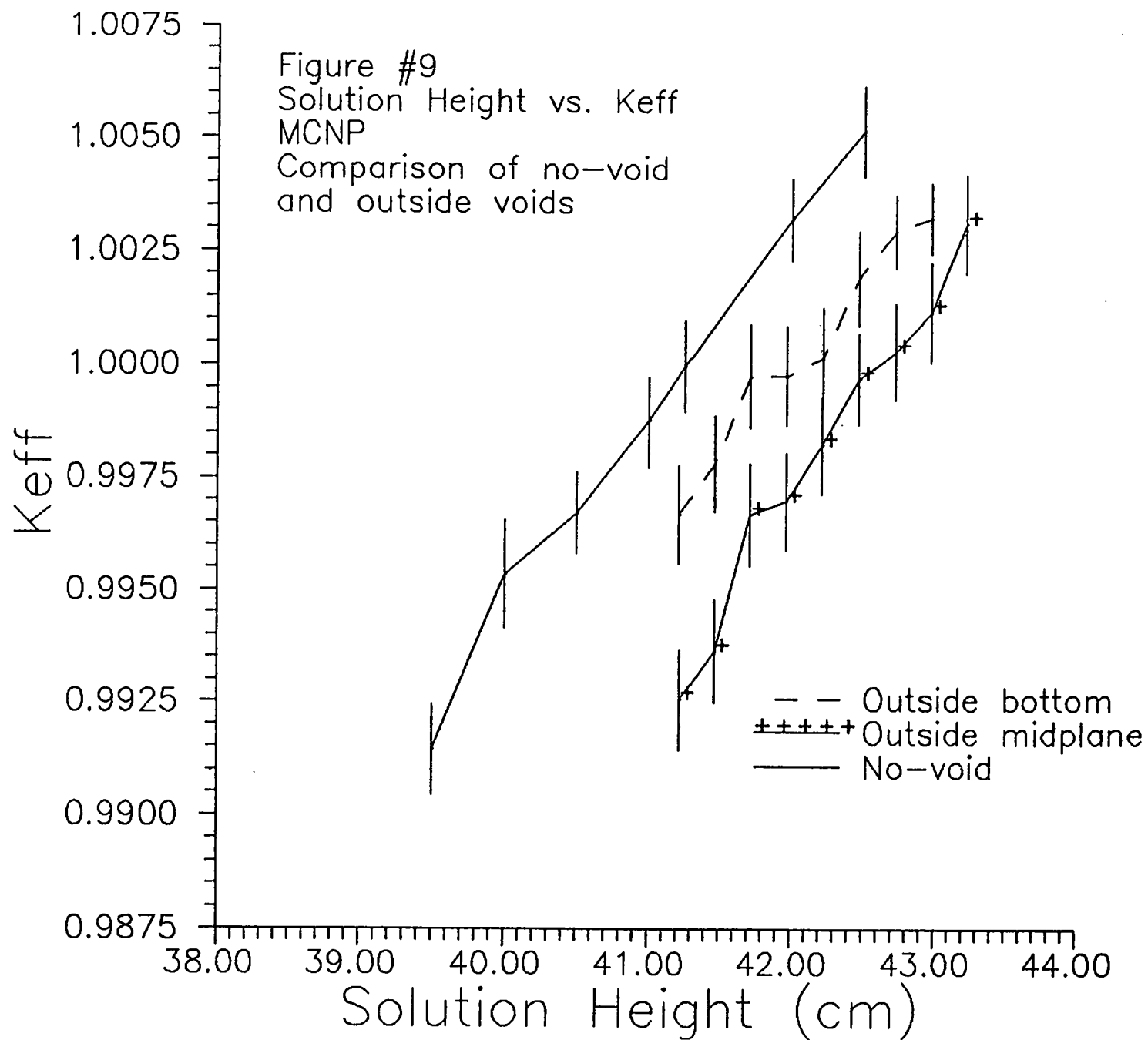


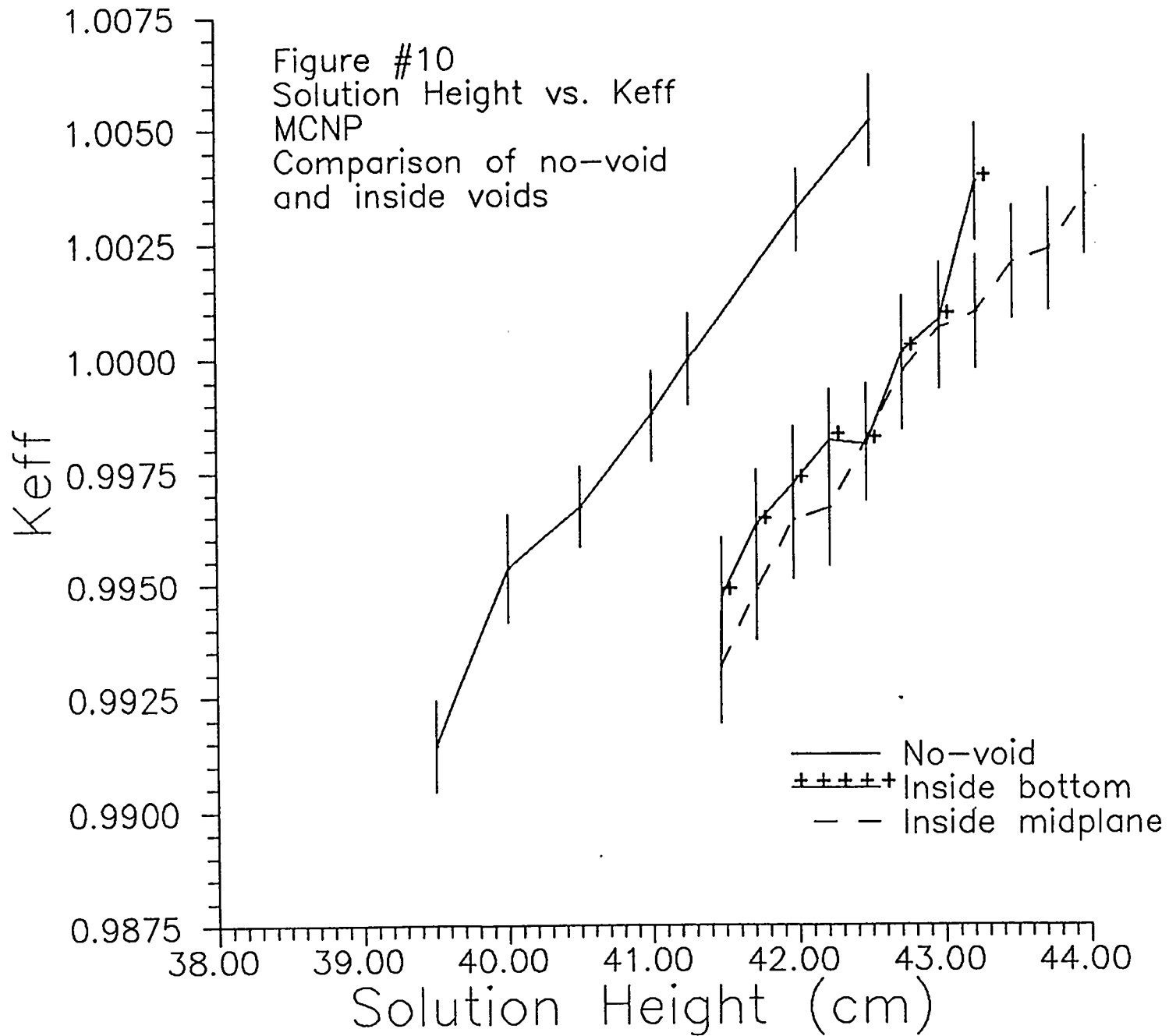


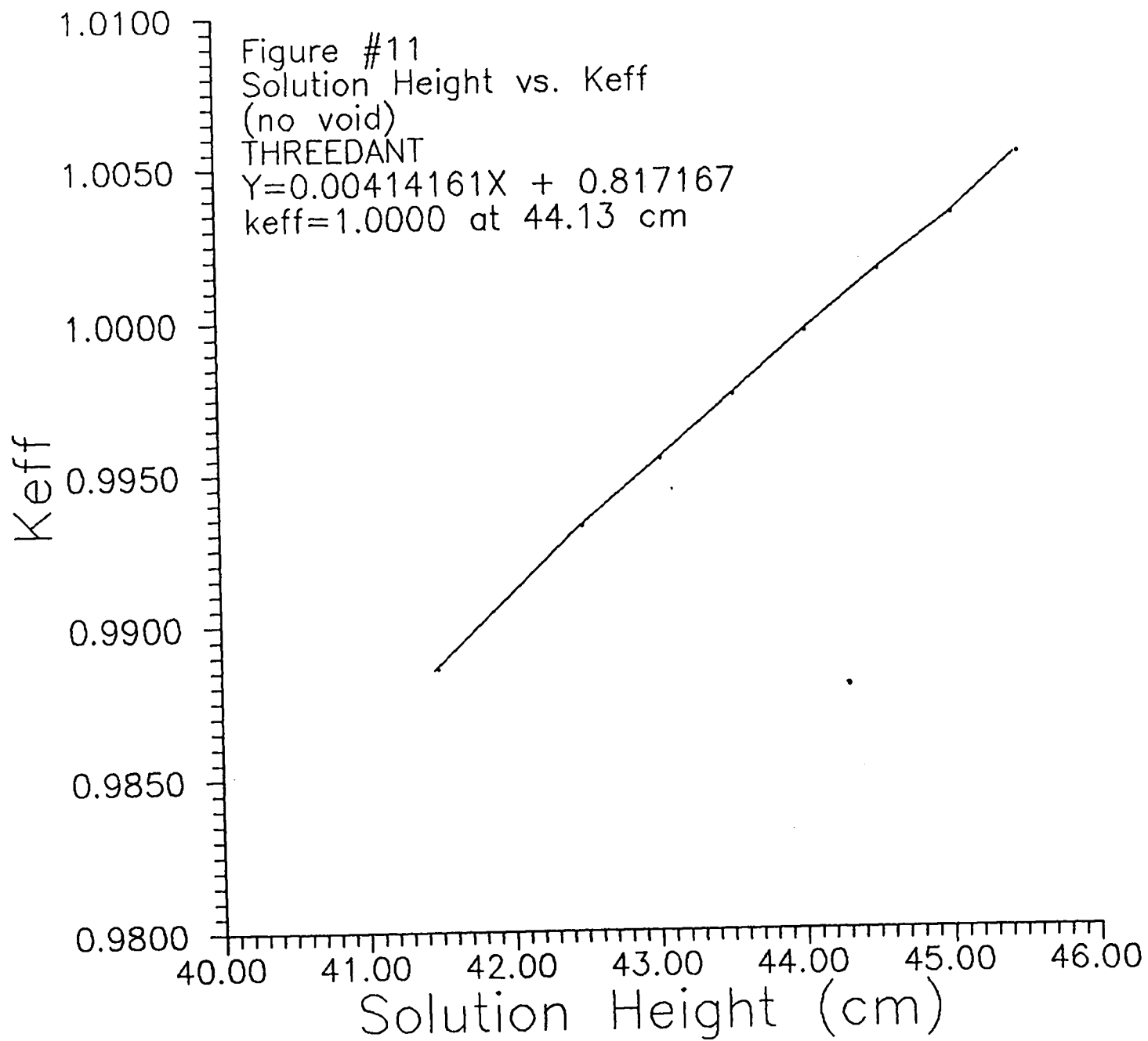


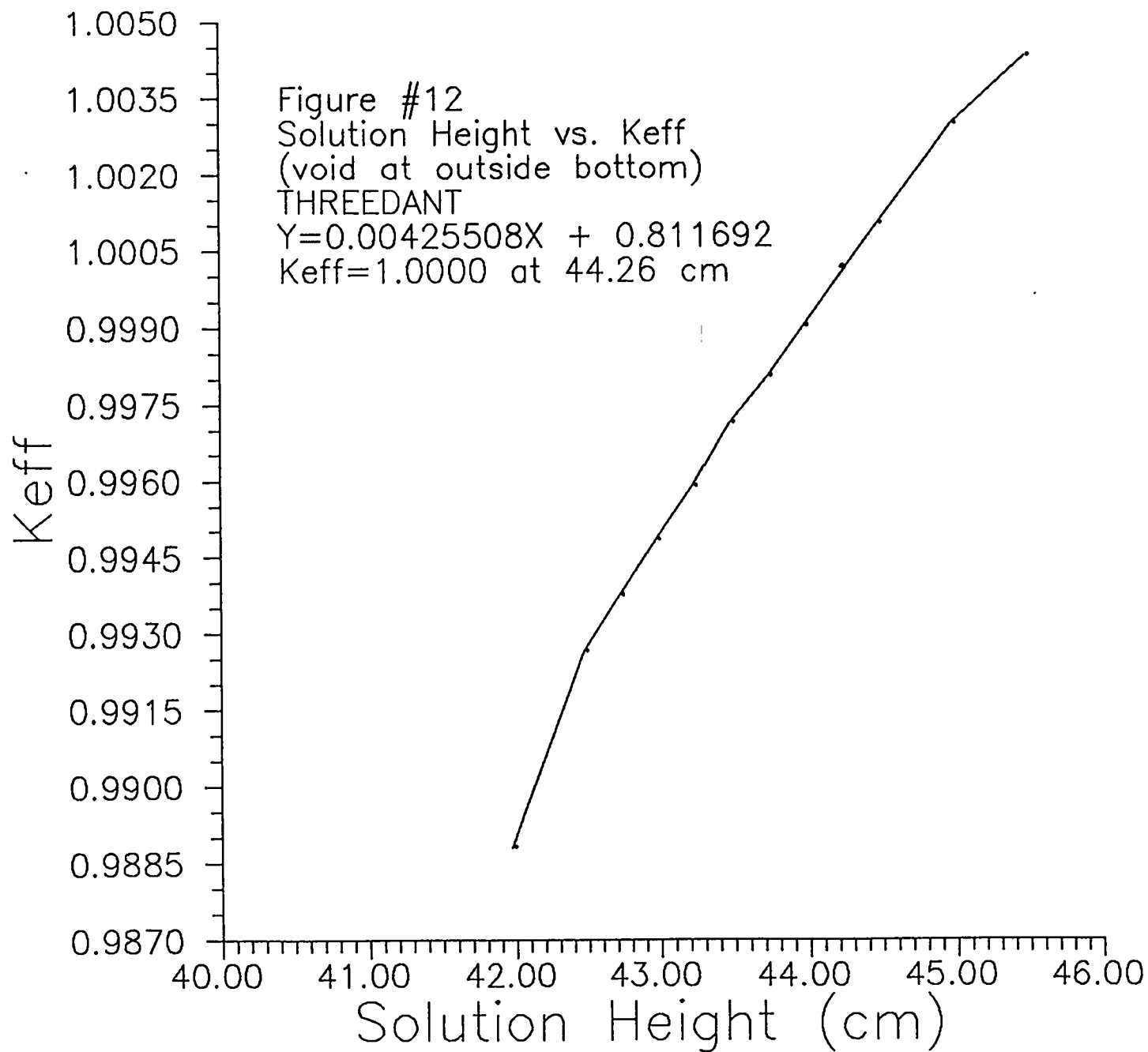




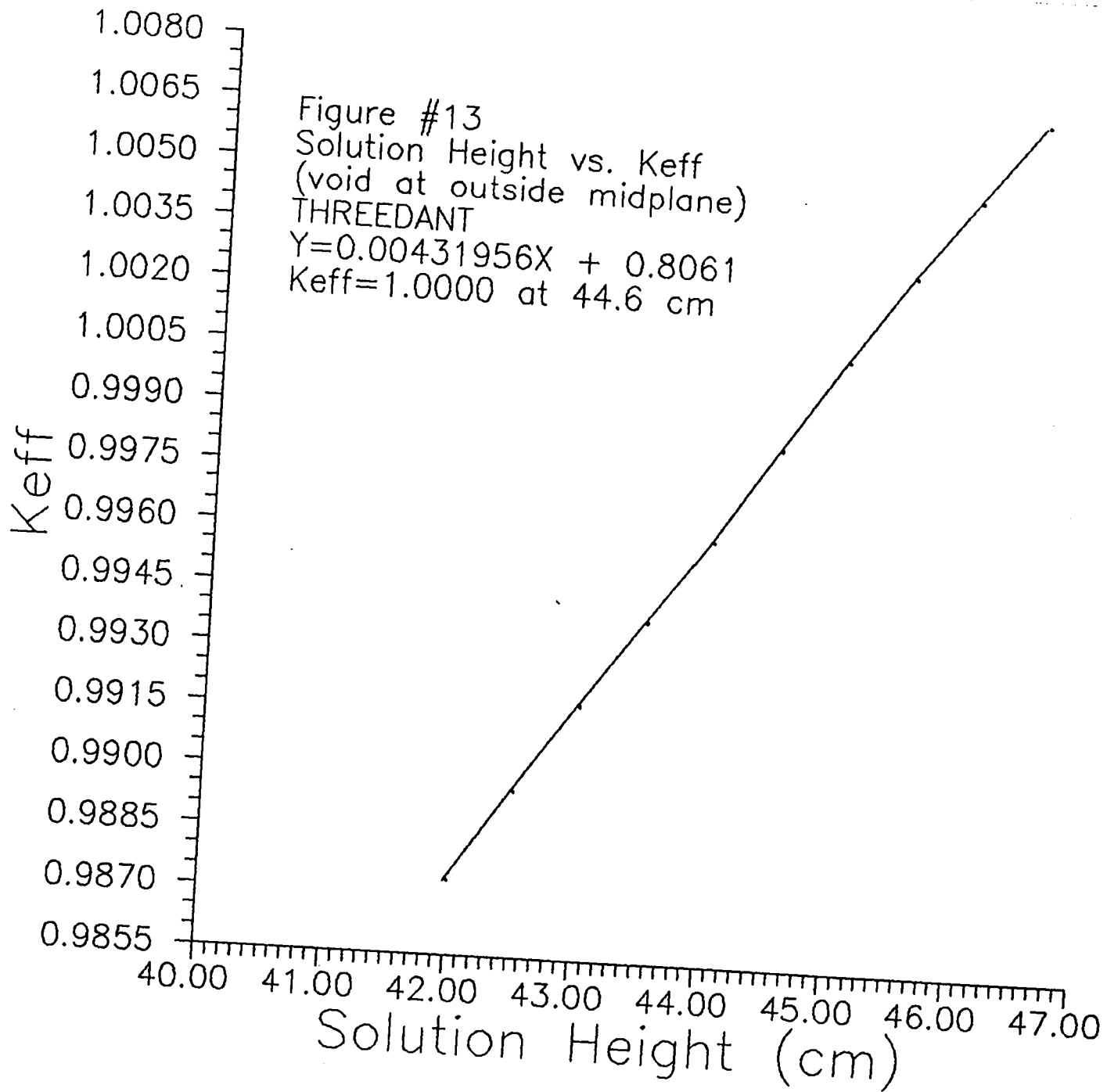


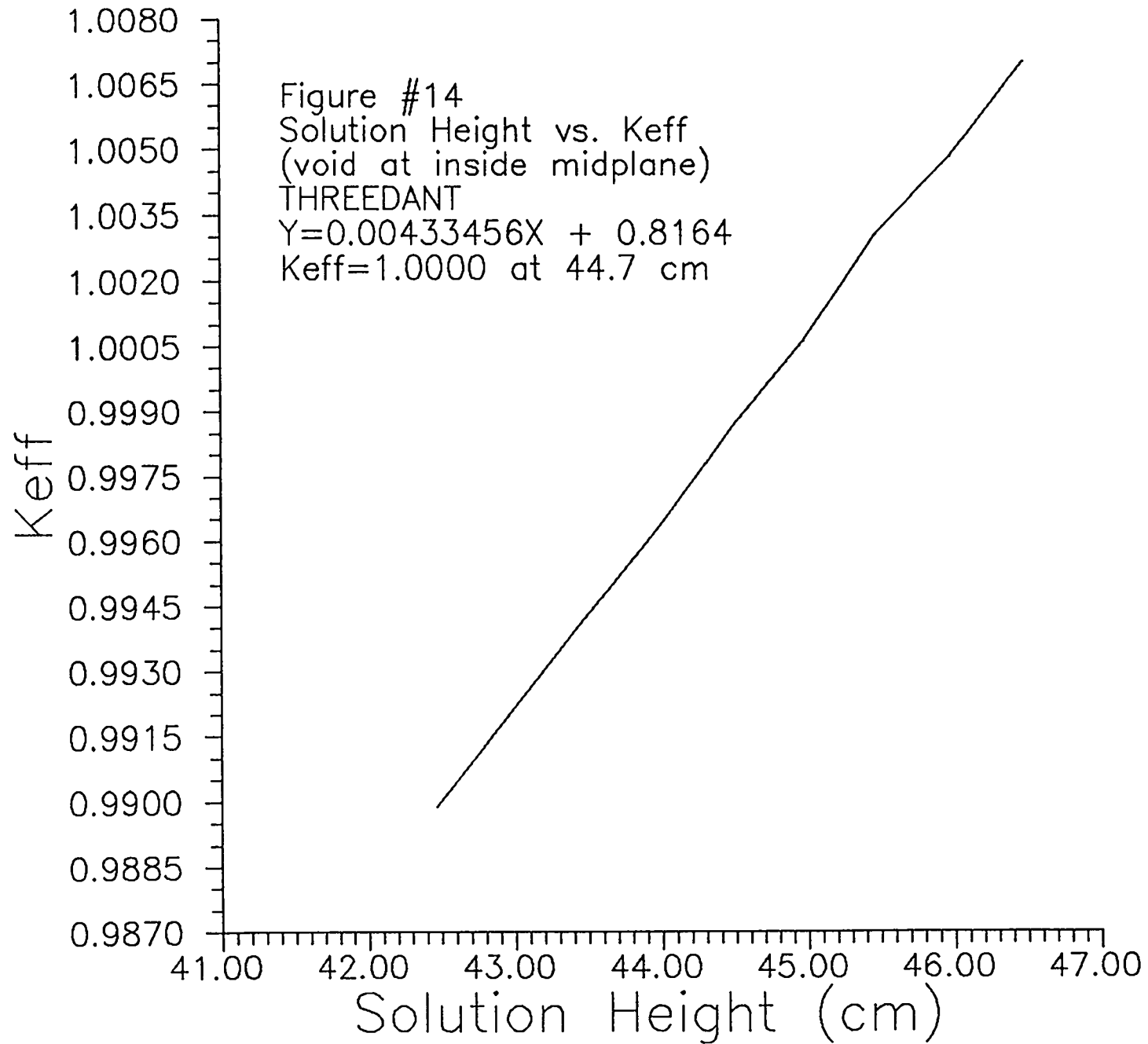


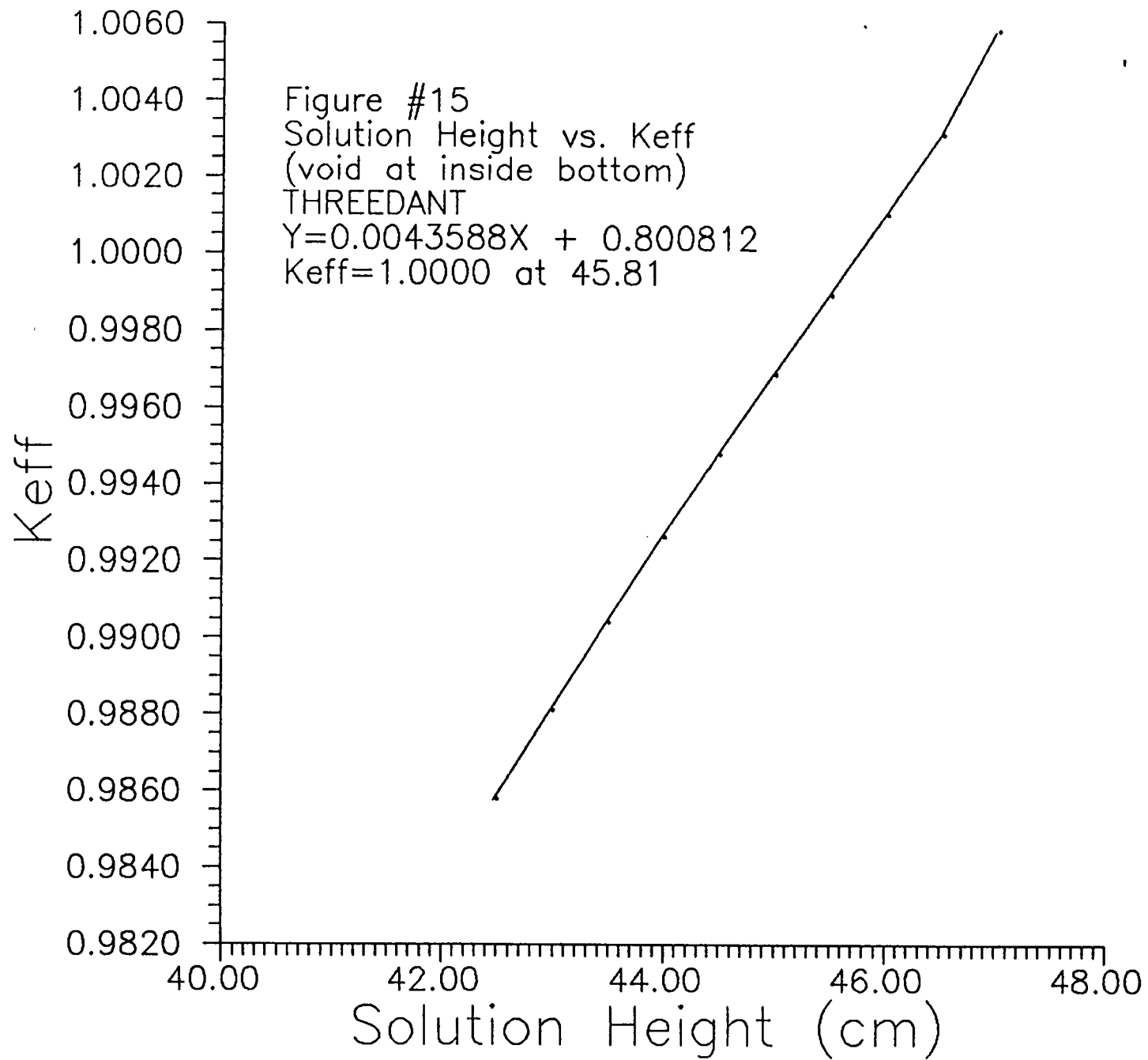


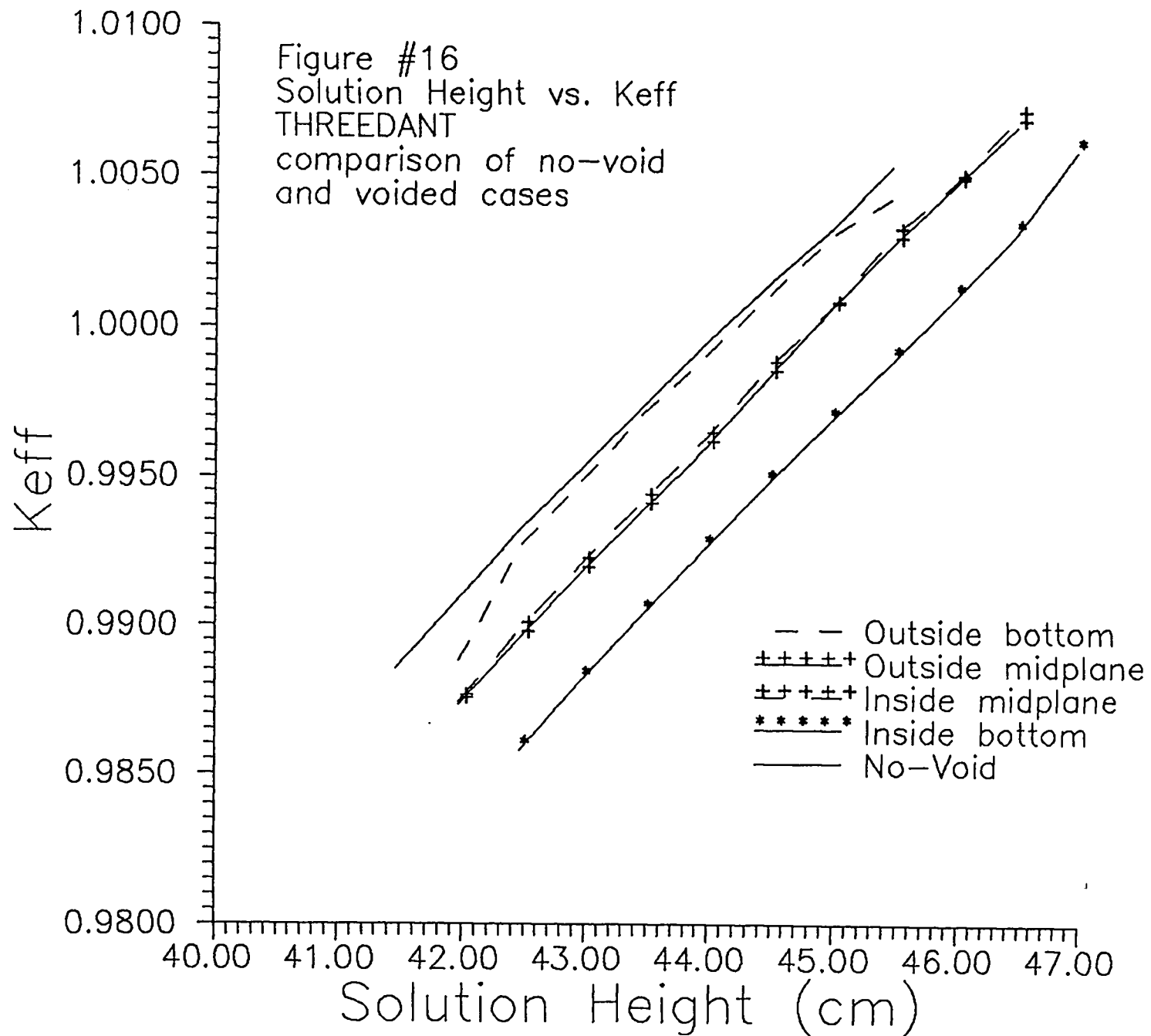


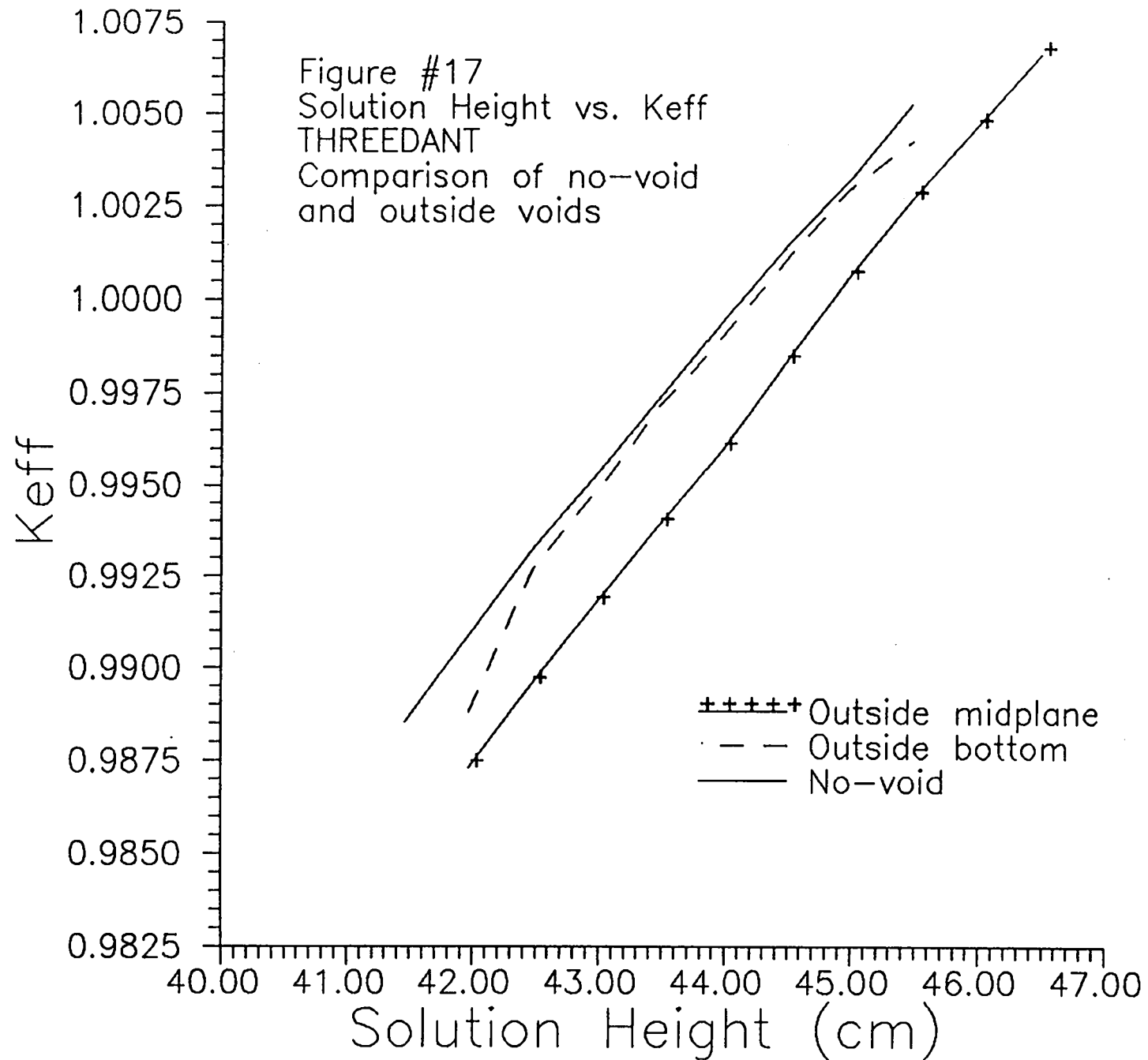
15











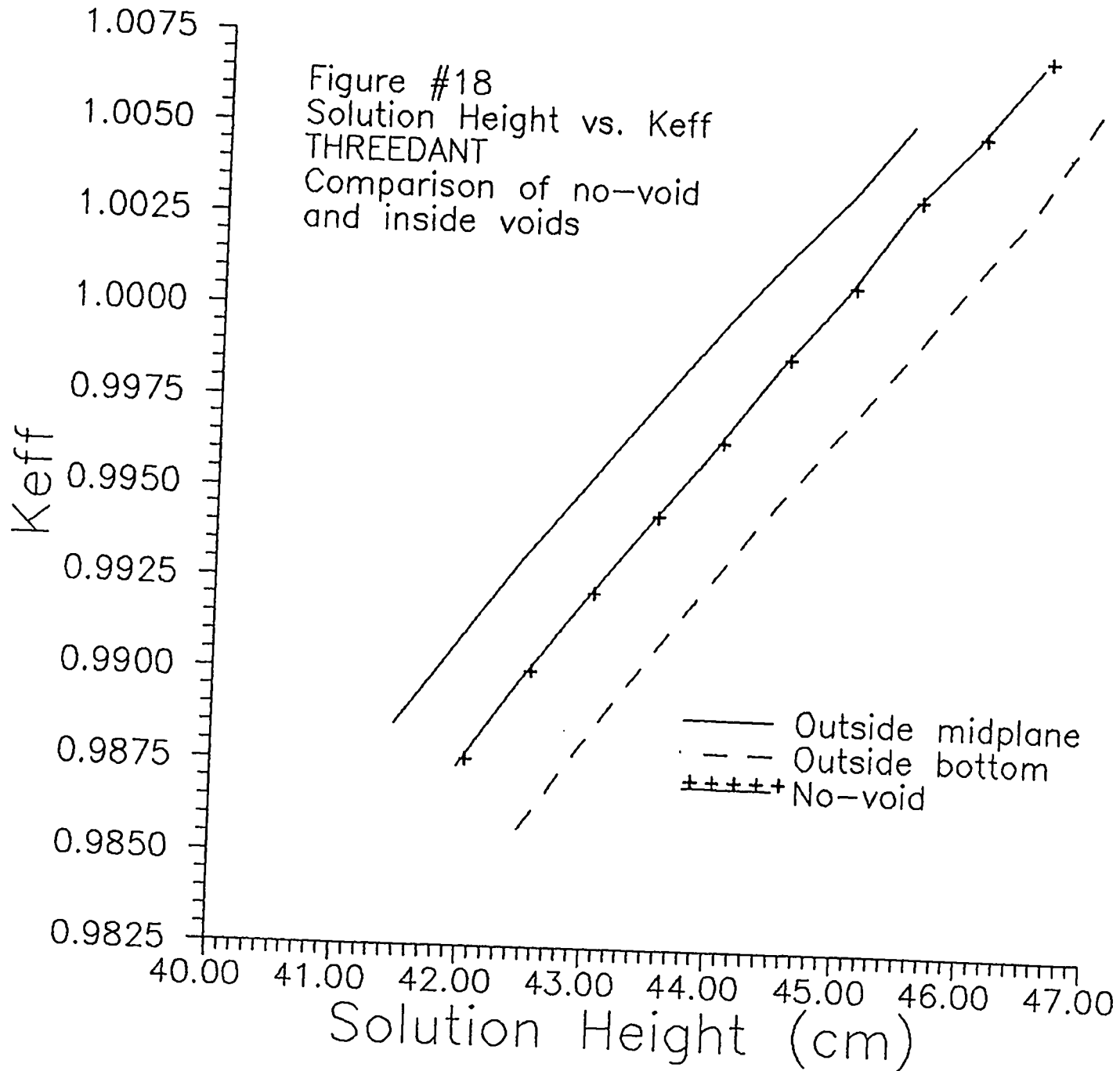
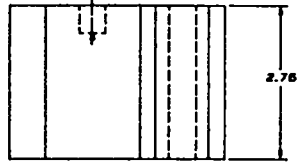
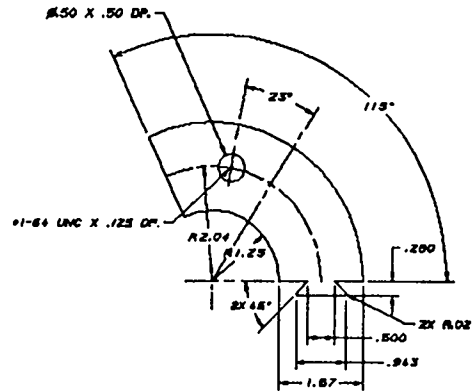
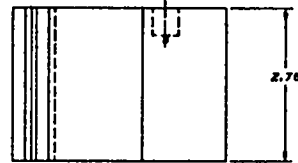
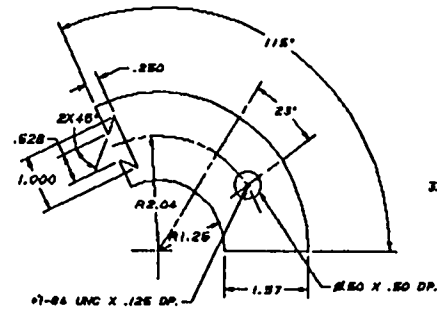


Figure #19

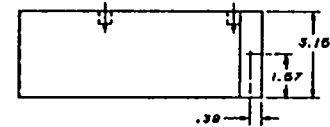
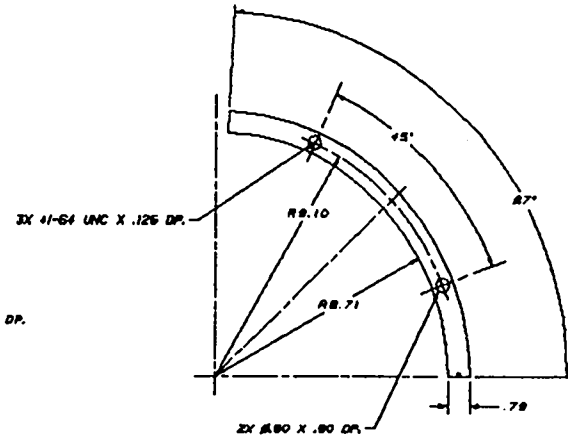
(AUTOCAD drawing of void for experiment)



3 INNER VOID MALE
SCALE 2/1



2 INNER VOID FEMALE
SCALE 2/1



1 OUTER VOID
SCALE 1/1

Appendix A

(MCNP input file)

```

lmcnp      version 4xe      ld=01/12/93      06/21/93 13:35:58
*****
06/21/93 13:35:58
inp=inbot outp=outtib
probid =

```

```

1-      Sheba II(complicated geometry)
2-      c      using thermal and prompt neutrons
3-      c      started history at pt out side of void
4-      c      changing shape from sphere to part of a cylinder
5-      c      using importance (splitting & roulette) to reduce variance
6-      c      Void placed at inside bottom
7-      c      Void thickness= 4 cm, ht=7 cm, arc length=230.211 degree
8-      c      Void placed with vol equiv to 7.5cm radius sphere
9-      c      void volume by 1767.144 cm^3
10-     c      solution ht increased by 0.9661019948 cm
11-     c      4 void templete
12-     1      10 9.36069-2 (-102 2 -101 -103 104 9)      $ U02F solution
13-     2      20 -7.9      (-4 1 2 -10)      $ ss,127cm walls,4826cm dia,12192cm high
14-     3      20 -7.9      (-4 5 -2 9)      $254cm ss tank bottom
15-     4      20 -7.9      (-4 -43 10 9)      $254cm ss tank top
16-     5      40 -2.7      (20 -21 25 -6)      $Al tank, 18,288cm dia, 254cm walls
17-     6      40 -2.7      (-21 9 22 -25)      $254cm Al tank bottom
18-     7      50 -1.12     (-62 63 -61)      $control rod material (mat 50)
19-     8      20 -7.9      (2 -61 62 -59)      $rod cladding
20-     9      0      (-7 -5 8)      $mt below rod, Below fluid ok be be void
21-     10     40 -2.7      (-9 7 -5 8)      $169.73cm Al tube under tank
22-     11     30 -2.2505 (11:15:-13:-17) (14 -12 18 -16 22 -6) $1524cm conc sle.
23-     12     30 -2.2505 (14 -12 18 -16 19 -22 9)      $1524cm thick con. base
24-     13     30 -2.2505 (14 -12 18 -16 23 -24)      $6096cm con. shield
25-     14     0      (4:43:-5) (-20 -6 5) #7 #8      $upper void
26-     15     0      (100)      $outside world, Should be VOID
27-     16     0      (-1 3 -10 9)      $void inside tank over fuel
28-     17     0      (-26 27 -28)
29-     18     20 -7.9      (26:-27:28) (-29 30 -31)      $$$ scram tank
30-     19     0      (-32 33 -34)      $u-fl in 2nd dump tank
31-     20     20 -7.9      (32:-33:34) (-35 36 -37)      $$$ scram tank
32-     21     20 -7.9      (38 -39 40 -41 42 -5 9)      $508cm ss support table
33-     22     0 -100      (-14:12:-18:16:-23:24) #6 #9 #10 #12
34-     23     20 -7.9      (20:6:-25) #11 #5      $outer void
35-     24     0      (38 -39 40 -41 44 -45 9)      $lower 508cm ss suppoprt
36-     25     0      (-20 25 -5) (29:-30:31) (35:-36:37) #9 #10 #21 #23
37-     26     0      (49:-50:51) (55:-56:57) #29      $lower void
38-     27     0      (-46 47 -48)      $u-fl in 3rd dump tank
39-     28     20 -7.9      (46:-47:48) (-49 50 -51)      $$$ scram tank
40-     29     0      (-52 53 -54)      $u-fl in 4th dump tank
41-     30     20 -7.9      (52:-53:54) (-55 56 -57)      $$$ dump tank
42-     31     0      (-20 25 -58 9)      $Down Below the solution, can
43-     32     20 -7.9      (7 -43 5 -9)      $glory hole wall
44-     33     70 100-100 (5 -43 -7 59)      $wall void      SHOULD NOT
45-     34     70 100-100 (-2 5 -59)      $void below out rod      SHOULD NO
46-     35     60 -1.60 (-62 2 -63)      $GRAPHITE FILLER 5080cm
47-     36     0      (61 -43 -59)      $void above out burst rod
48-     c
49-     c      void area @ (r,theta,z) 23.13,0,2.27
50-     35     70 100-100 (9 -102 103 -104 2 -101) $cylinder slice @bottom cor.
51-     c      70 100-100 ( ) $cylinder slice @midplane cor.
52-     c
53-     39     10 9.36069-2 (102 -1 2 -101 -103 104) $Area diag. from "35" void
54-     40     10 9.36069-2 (101 -3 -1 102 -103 104) $Area above cell 39, diag in x
55-     41     10 9.36069-2 (101 -3 -1 102 -103 -104) $area above and next to void "35"
56-     42     10 9.36069-2 (101 -3 -1 102 103 -104) $area above void "35", good for g
57-     43     10 9.36069-2 (101 -3 -1 102 103 104) $area above and next to void "35"
58-     44     10 9.36069-2 (101 -3 -102 9 -103 104) $area inside cell 40
59-     c
60-     45     10 9.36069-2 (-102 2 -101 -103 -104 9) $area insdie 48
61-     46     10 9.36069-2 (102 2 -101 103 -104 -1) $area outside void area "35" goo
62-     47     10 9.36069-2 (-102 2 -101 103 104 9) $area inside 49
63-     48     10 9.36069-2 (102 -1 2 -101 -103 -104) $area outside 45, next to void "
64-     49     10 9.36069-2 (102 -1 2 -101 103 104) $area outside 47, next to void
65-     50     10 9.36069-2 (101 -3 -102 9 -103 -104) $area inside cell 41
66-     51     10 9.36069-2 (101 -3 -102 9 103 -104) $area inside cell 42
67-     52     10 9.36069-2 (101 -3 -102 9 103 104) $area inside cell43

```

68-					
69-	1	cz 24.13	\$i.r of main tank		
70-	2	pz 1.27	\$lower fluid height		
71-	3	pz 42.7361019948	\$upper fluid height (1.27+0.9661019948+40.5)		
72-	4	cz 25.40	\$o.r of main tank		
73-	5	pz -1.27	\$bottom of ss tank		
74-	6	pz 130.73	\$top of Al tank		
75-	7	cz 2.54	\$i.r of central thimble		
76-	8	pz -171.0			
77-	9	cz 3.175	\$o.r of central thimble		
78-	10	pz 126.44	\$top of ss. vessel, bottom is s2		
79-	11	px 95.			
80-	12	px 105.24			
81-	13	px -95.			
82-	14	px -105.24			
83-	15	py 95.			
84-	16	py 105.24			
85-	17	py -95.			
86-	18	py -105.24			
87-	19	pz -169.01			
88-	20	cz 91.44	\$i.r of Al tank		
89-	21	cz 93.98	\$o.r of Al tank		
90-	22	pz -153.77			
91-	23	pz 138.43			
92-	24	pz 199.39			
93-	25	pz -151.23			
94-	26	1 c/x 20.	-32. 10.16		
95-	27	1 px -58.43			
96-	28	1 px 58.43			
97-	29	1 c/x 20.	-32. 11.43		
98-	30	1 px -59.67			
99-	31	1 px 59.67			
100-	32	1 c/x -20.	-32. 10.16		
101-	33	1 px -58.43			
102-	34	1 px 58.43			
103-	35	1 c/x -20.	-32. 11.43		
104-	36	1 px -59.68			
105-	37	1 px 59.68			
106-	38	px -50.			
107-	39	px 50.			
108-	40	py -50.			
109-	41	py 50.			
110-	42	pz -6.35			
111-	43	pz 128.98			
112-	44	pz -117.			
113-	45	pz -111.92			
114-	46	2 c/x 20.	-80. 10.16		
115-	47	2 px -28.42			
116-	48	2 px 88.42			
117-	49	2 c/x 20.	-80. 11.43		
118-	50	2 px -29.67			
119-	51	2 px 89.67			
120-	52	2 c/x -20.	-80. 10.16		
121-	53	2 px -28.43			
122-	54	2 px 88.43			
123-	55	2 c/x -20.	-80. 11.43		
124-	56	2 px -29.68			
125-	57	2 px 89.68			
126-	58	pz -146.43			
127-	59	cz 2.2225	\$444.5cm o.d. of rod		
128-	61	pz 102.87	\$top of rod in out pos.		
129-	62	cz 2.143125	\$id of rod cladding		
130-	63	pz 52.07			
131-	100	so 440.	\$sphere that comprises outside world		
132-	c		Beginning of the void treatment		
133-	101	pz 8.27			
134-	102	cz 7.175	\$inside cylinder		
135-	103	py 0	\$0 degree plane		
136-	104	p 17.1488853698	-21.169948443 0 37.973650912	\$approx a 230.211 degree	
137-					
138-	*tr1	0. 0. 0. 15. 90. 75. 90. 0. 90. 105. 90. 15. 1			
139-	*tr2	0. 0. 0. 15. 90. 105. 90. 0. 90. 75. 90. 15. 1			
140-	mode n				
141-	imp:n	1 13r 0 1 18r 3 1 1 1 2 1 1 1 2 1 2 2 1 1 1			
142-	c	vol 11j 674847. 8j 18724.0 1j 18724. 1798160. 10j			
143-	m10	92235.50c 1.319-4 92238.50c 2.499-3			
144-		92236.51c 1.316-6			
145-		1001.50c 5.354-2 8016.50c 3.210-2 9019.51c 5.334-3			
146-	m20	26000.55c -6.950-1 24000.50c -1.9-1 28000.50c -9.5-2			
147-		25055.51c -2.0-2			
148-	m30	1001.50c -.004532 8016.50c -.512597 11023.51c -.011553			
149-		12000.51c -.003866 13027.50c -.035548 14000.51c -.360364			
150-		19000.51c -.014219 20000.51c -.043546 26000.55c -.013775			
151-	m40	13027.50c 1.0			
152-	m50	1001.50c 5.55-2 6000.50c 2.8164-2 5010.50c 3.74-3			
153-		5010.50c 1.496-2			

```
154-      m60      6000.50c 1.0
155-      m70      5010.50c 1
156-      c
157-      totnu no
158-      c
159-      c      thermal treatment
160-      c
161-      mt10 lwtr.01t
162-      c
163-      kcode 2000. 1.0 10 350
164-      c      ksrc 05.0 -5. 9.0 0. 5.01 16. -5. 5. 16. 0. -5. 30. 14. 14. 3.
165-      print
166-
```


3 ahead number of title cards to follow
0 notty 0/1 no/yes suppress on-line terminal output
0 nolist 0/1 no/yes suppress input listing

* SHIMA-II Critical reactor
* Dirlow=6.35(3.175)cm 1d=48.26(24.13)cm
* RROCA=44.5cm * .9661019948 cm

key end block i read

...block i - controls and dimensions...

...dimensions (array name = dime*)...

15 lgeom 14/15 x-y-z/ r-x-theta
16 ngroup number of energy groups
8 lms angular quadrature order
118 niso number of input isotopes (from isotas, groups, or cards)
5 wt number of permanent materials
3 nzone number of zones
6 lm number of coarse mesh x intervals
34 it number of fine mesh intervals
7 jm number of coarse mesh y intervals
36 jt number of fine mesh y intervals
3 km number of coarse mesh z intervals
13 kt number of fine mesh z intervals

...storage...
maxlon= 6000000
maxscm= 1100000

key end block ii read-geom

15 lgeom 1/2/3/4/7/8/9/11/14

key end block iii read-ms

...block iii - cross section library...

...library source...
lib=exlib

...energy structure...

group	chi	wel	lower bound	upper bound	group	chi	wel	lower bound	upper bound
1	2.04000E-01	2.83000E+01	3.00000E+06	1.00000E+08	9	0.00000E+00	2.06000E-01	1.00000E+02	5.30000E+02
2	3.44000E-01	1.89000E+01	1.40000E+06	3.00000E+08	10	0.00000E+00	1.01000E-01	3.00000E+01	1.00000E+02
3	1.68000E-01	1.47000E+01	9.00000E+05	1.40000E+06	11	0.00000E+00	3.66000E-02	1.00000E+01	3.00000E+01
4	1.80000E-01	1.10000E+01	4.00000E+05	9.00000E+05	12	0.00000E+00	3.19000E-02	3.00000E+00	1.00000E+01
5	9.00000E-02	6.70000E+00	1.00000E+05	4.00000E+05	13	0.00000E+00	1.79000E-02	1.00000E+00	3.00000E+00
6	1.40000E-02	2.70000E+00	1.70000E+04	1.00000E+05	14	0.00000E+00	1.09000E-02	4.00000E-01	1.00000E+00
7	0.00000E+00	1.14000E+00	3.00000E+03	1.70000E+04	15	0.00000E+00	6.06000E-03	1.00000E-01	4.00000E-01
8	0.00000E+00	4.80000E-01	5.50000E+02	3.00000E+03	16	0.00000E+00	2.18000E-03	0.00000E+00	1.00000E-01

last neutron group(lng) is number 16

0 habs -1/0/1 - adjust absorption/no/adjust self scatter to force xs balance

...edit position names...

position edname
1 chl
2 awsigf
3 total
4 abs
5 n-fiss

...isotope names and numbers from library...

number	name	number	name	number	name	number	name
1	al	25	240-6	49	239-12	73	238-10
2	b	26	240-7	50	239-13	74	238-11
3	be	27	240-8	51	239-14	75	238-12
4	c	28	240-9	52	239-15	76	238-13
5	cd	29	240-10	53	239-16	77	238-14
6	cl	30	240-11	54	th	78	238-15
7	ga	31	240-12	55	u233	79	238-16
8	fl9	32	240-13	56	233-1	80	xr
9	fe	33	240-14	57	233-2	81	n
10	h	34	240-15	58	233-3	82	nb
11	h	35	240-16	59	233-4	83	235-yr
12	i16	36	240-17	60	233-5	84	235-1r
13	i17	37	240-18	61	233-6	85	235-2r
14	me	38	239-1	62	233-7	86	235-3r
15	na	39	239-2	63	233-8	87	235-4r
16	ni	40	239-3	64	233-9	88	235-5r
17	o16	41	239-4	65	233-10	89	235-6r
18	pu239	42	239-5	66	233-11	90	235-7r
19	pu240	43	239-6	67	233-12	91	235-8r
20	240-1	44	239-7	68	w239	92	235-9r
21	240-2	45	239-8	69	w238	93	235-10r
22	240-3	46	239-9	70	w237b	94	238-1r
23	240-4	47	239-10	71	238-6	95	238-2r
24	240-5	48	239-11	72	238-9	96	238-3r

key end card libe read

key end block iv read-mats

...mixing instructions...

mix comp density comp density etc.


```

0 0.000E+00          0.000E+00          0.000E+00
1 2.143E+00      2 1.072E+00      2.540E+00      2 1.270E+00      3.194E-01      5 6.388E-02
2 2.540E+00      1 3.969E-01      9.547E+00      13 9.385E-01      5.000E-01      8 2.237E-02
3 3.175E+00      2 3.175E-01      4.801E+01      24 1.603E+00
4 7.175E+00      9 4.448E-01      5.334E+01      4 1.333E+00
5 2.413E+01      16 1.060E+00      1.060E+02      7 7.529E+00
6 2.540E+01      4 3.175E-01      1.277E+02      3 7.223E+00
7 1.302E+02      3 8.467E-01

```

...cross section related data from file namrn 00000011890 version 1 ...

1 fuel 2 steel 3 strlrs 4 follow 5 filler

...iteration controls and criteria...

iteration criteria

		transport inners		
critrion	quantity to test	value	action taken if value exceeded	
liti	- inner iteration count until near lambda (i.e. fission source) convergence	1	terminates inners	
litn	- inner iteration count when near lambda (i.e. fission source) convergence	30	terminates inners	
epsi	- fractional ptwise flux change per inner	1.00E-04	does another inner	

		diffusion sub-outers		
critrion	quantity to test	value	action taken if value exceeded	
sltd	- sub-outer iteration count	40	terminates sub-outers	
epsd	- diffusion lambda=1.0 (see note below)	1.00E-04	does another sub-outer	
epfd	- fractional ptwise fission change per sub-outer (see note below)	1.00E-04	does another sub-outer	

note: eps, when the problem is finally converged, will equal epsi, the value shown above, however, vary in the iteration process, a larger value may be used to avoid unnecessary iterations.

final convergence criteria

critrion	quantity to test	value	action taken if value exceeded
sltm	- outer iteration count	20	quits with error message
epsf	- transport lambda=1.0	1.00E-04	does another outer

...flux and eigenvalue convergence as monitored by threedant...

key start iteration monitor

cpu time	outer	diffusion	k-eff	max ptwise	max ptwise	inners		
(sec)	no. inners	sub-outers	eigenvalue	lambda-1	flux change	fiss change	converged	
62.43	0							
1193.61	1	0	3	1.00206438	5.39279E-03	0.00000E+00	0.00000E+00	**ne**
3920.64	2	32	2	1.00621614	4.67099E-03	1.34000E+00	8.74907E-01	**ne**
6729.01	3	32	4	0.99982788	-6.48419E-03	1.83886E-01	6.48833E-02	**ne**
9347.47	4	32	2	0.99988774	7.92676E-05	2.23293E-01	1.98724E-02	**ne**
12024.	5	32	3	0.99982633	3.74005E-05	1.84862E-01	8.63697E-03	**ne**
14622.	6	32	3	0.99981790	-7.94837E-06	1.24028E-01	1.94198E-03	**ne**
17020.	7	32	3	0.99981318	-4.43695E-06	1.80151E-02	1.30041E-03	**ne**
19399.	8	32	3	0.99980513	-7.57677E-06	7.67103E-03	1.74833E-03	**no**

-- Inner iteration summary for outer iteration no. 9 --

group	iter	per	max flux	at
group	group	change	mesh	
1	9	0.68E-04	6, 46, 12	
2	6	0.94E-04	14, 56, 12	
3	9	0.73E-04	13, 56, 13	
4	6	0.67E-04	13, 56, 13	
5	9	0.75E-04	12, 56, 13	
6	6	0.88E-04	10, 47, 13	
7	19	0.84E-04	1, 52, 13	
8	10	0.93E-04	34, 53, 13	
9	8	0.98E-04	1, 52, 13	
10	16	0.80E-04	1, 52, 13	
11	10	0.91E-04	1, 52, 13	
12	11	0.95E-04	8, 56, 5	
13	10	0.70E-04	3, 46, 13	
14	6	0.91E-04	1, 51, 13	
15	12	0.86E-04	24, 56, 13	
16	11	0.85E-04	2, 33, 5	

cpu time	outer	diffusion	k-eff	max ptwise	max ptwise	inners		
(sec)	no. inners	sub-outers	eigenvalue	lambda-1	flux change	fiss change	converged	
29247.	9	130	2	0.99990089	-4.07802E-04	9.82965E-05	1.52119E-06	yes

**** some acceleration inhibited ****
 ***** all convergence criteria satisfied *****

particle balance = -1.65536E-03 total inners all outers = 375

...group edit and balances upon convergence...

...title---SHEXA-II Critical reactor

...system balance tables... (neutrons only)

*key start balance table *

gp	source	fission source	absorption	in scatter	self scatter	out scatter	net leakage
1	0.000000E+00	2.836677E+03	7.3922914E+01	6.3646629E-11	8.7760250E+02	2.2169736E+03	3.4432648E+02
2	0.000000E+00	4.444827E+03	6.4899312E+01	1.3032098E+03	2.6144644E+03	3.0089688E+03	6.7629977E+02
3	0.000000E+00	2.1715381E+03	1.1711702E+01	2.3175653E+03	1.9928162E+03	4.1918804E+03	3.2567694E+02
4	0.000000E+00	2.3266478E+03	1.6999939E+01	4.6305395E+03	4.3743173E+03	6.4973092E+03	4.4316340E+02
5	0.000000E+00	1.1633240E+03	2.0883811E+01	7.4288945E+03	7.7325637E+03	8.1463158E+03	4.1158900E+02
6	0.000000E+00	1.8096151E+02	3.6757727E+01	8.4944573E+03	8.5181038E+03	8.5782353E+03	2.6246209E+02
7	0.000000E+00	0.000000E+00	4.4066335E+01	8.4936149E+03	8.0274141E+03	8.3072754E+03	1.4029564E+02
8	0.000000E+00	0.000000E+00	9.0430599E+01	8.2305010E+03	7.3645355E+03	8.0300189E+03	1.3009571E+02
9	0.000000E+00	0.000000E+00	2.3321938E+02	8.0729447E+03	7.1981129E+03	7.7114652E+03	1.0724643E+02
10	0.000000E+00	0.000000E+00	3.1325194E+02	4.6684210E+03	3.6487468E+03	6.2644040E+03	1.1746904E+01
11	0.000000E+00	0.000000E+00	2.7486203E+02	6.0956441E+03	2.8738737E+03	5.7584500E+03	4.2333642E+01
12	0.000000E+00	0.000000E+00	4.6251840E+02	6.1700026E+03	3.1206341E+03	5.6462985E+03	6.1189622E+01
13	0.000000E+00	0.000000E+00	9.0838558E+01	5.3386736E+03	2.6186824E+03	3.4039891E+03	5.3649277E+01
14	0.000000E+00	0.000000E+00	1.1847352E+02	4.9307960E+03	2.8951303E+03	4.7703505E+03	4.1962646E+01
15	0.000000E+00	0.000000E+00	7.7024338E+02	5.8829615E+03	2.2682916E+03	5.1046977E+03	8.8263185E+01
16	0.000000E+00	0.000000E+00	6.9253749E+03	7.0480954E+03	1.6896558E+04	2.8230716E+03	1.3527177E+02
tot	0.000000E+00	1.2925822E+04	9.5826044E+03	9.1630321E+04	2.5356728E+05	9.1630363E+04	3.3469466E+03

gp	right leakage	horizontal leakage	top leakage	vertical leakage	front leakage	fr-back leakage	particle balance
1	2.8411089E-02	2.8411089E-02	5.5065520E+00	5.0215188E+01	4.1063144E-04	4.1063144E-04	-8.4837171E-05
2	9.1351387E-02	9.1351387E-02	1.1314388E+01	1.0278500E+02	9.0574773E-04	9.0574773E-04	-8.0748975E-05
3	2.7049885E-02	2.7049885E-02	5.9968250E+00	5.5177368E+01	3.5036781E-04	3.5036781E-04	-3.6426071E-05
4	3.4752453E-02	3.4752453E-02	8.1273325E+00	7.5636461E+01	4.0827142E-04	4.0827142E-04	-3.4442568E-05
5	3.4122708E-02	3.4122708E-02	7.3796754E+00	7.0061097E+01	6.7357403E-04	6.7357403E-04	-3.0673997E-05
6	1.1808408E-02	1.1808408E-02	4.4887945E+00	4.4597668E+01	3.7128342E-04	3.7128342E-04	-2.7465047E-05
7	1.1998694E-02	1.1998694E-02	2.2107815E+00	2.0308677E+01	2.0297414E-05	2.0297414E-05	-1.3707021E-04
8	1.1046314E-02	1.1046314E-02	1.1023138E+00	1.8632176E+01	3.7763744E-04	3.7763744E-04	-5.3628666E-06
9	9.2815624E-01	9.2815624E-01	1.6942319E+00	1.3428797E+01	1.3967398E-04	1.3967398E-04	-1.7059950E-07
10	6.1473619E-01	6.1473619E-01	1.1292036E+00	1.0293255E+01	3.0828276E-04	3.0828276E-04	-1.0794568E-07
11	5.1480743E-01	5.1480743E-01	9.4148950E-01	8.8730341E+00	6.3356184E-05	6.3356184E-05	-1.2517488E-07
12	3.2594960E-01	3.2594960E-01	9.1761528E-01	8.4346039E+00	5.8403672E-05	5.8403672E-05	-3.0452546E-07
13	4.4542894E-01	4.4542894E-01	7.4315690E-01	7.3062954E+00	8.8159519E-05	8.8159519E-05	-6.1089518E-07
14	3.4524275E-01	3.4524275E-01	5.5957437E-01	5.4382490E+00	1.4428266E-04	1.4428266E-04	-1.0421801E-07
15	7.7889509E-01	7.7889509E-01	9.4153520E-01	1.0353208E+01	4.6797368E-04	4.6797368E-04	-3.7141143E-06
16	1.1264068E-02	1.1264068E-02	9.3228693E-01	1.0866101E+01	4.1710906E-04	4.1710906E-04	-1.2463237E-06
tot	2.8293134E+03	2.8293134E+03	5.5062758E+01	5.1562815E+02	5.3276019E-03	5.3276019E-03	-1.6353647E-05

Multigrid work units... Total= 10430.84 WD.
 By group...
 1 608.75 2 568.11 3 320.82 4 501.47 5 301.84 6 478.85 7 730.50 8 582.40 9 618.40
 10 740.48 11 662.37 12 743.45 13 830.38 14 837.52 15 746.43 16 737.97
 Multigrid average convergence rate by group...
 1 0.8832 2 0.8974 3 0.8173 4 0.8916 5 0.8582 6 0.8257 7 0.7408 8 1.0758 9 0.7588
 10 0.7713 11 0.8120 12 0.8538 13 1.8563 14 0.9344 15 2.0374 16 0.9147
 timing info... tswp,tdss,trelx,tput3,tintrp=21420.30 6619.71 3446.05 562.93 394.85 seconds.

Integral summary information
 summary integral-k-eff 9.9980089E-01
 integral-source-1 neutron 0.0000000E+00
 integral-fission-1 neutron 1.2925822E+04
 integral-absorption-1 neutron 9.5826044E+03
 integral-in-scak-1 neutron 9.1630321E+04
 integral-self-scak-1 neutron 2.5356728E+05
 integral-out-scak-1 neutron 9.1630363E+04
 integral-net lkage-1 neutron 3.3469466E+03
 integral-right lkage-1 neutron 2.8293134E+03
 integral-horizontal lkage-1 neutron 2.8293134E+03
 integral-top lkage-1 neutron 5.5062758E+01
 integral-vertical lkage-1 neutron 5.1562815E+02
 integral-front lkage-1 neutron 5.3276019E-03
 integral-fr-back lkage-1 neutron 5.3276019E-03
 integral-particle bal-1 neutron -3.2033493E-04

...interface file rflux written..

...interface file snocs written..

threads: iteration time, mins 4.8754E+02

edit run on with solver version 05-24-93*product release 2.3a machine jesabel

...edit output...

...block vi - edit specification data...

*key start edit output *

cross section balancing (balke.ne.0)
 or
 transport correction (trccorrdiag, cswaro, or hns)
 will NOT be reflected in edits

```

...input control integers...
1 pted 0/1 no/yes - point edits desired
0 tned 0/1 no/yes - zone edits desired
0 ajed 0/1 direct/adjoint edit(see rflux/atflux file)
0 isped 0/1/2/3 print totals only/print broad groups only/save as 1/print all groups and totals
0 bywslp 0/1 no/yes - multiply point reaction rates by mesh volumes
0 rslfx 0/1 no/yes - write the rslfx file (zone average flux file)
0 rsmflx 0/1 no/yes - write the rsmflx file (zone average flux moments file)

```

```

...floating parameters...
0.000000E+00 power 0/p no/normalize all results, including flux files, to p megawatts
2.100000E+02 mevper mev per fission (default: 210 mev)

```

...energy related edit information...

```

16 number of fine neutron groups
0 number of fine gamma groups
16 total number of fine groups
16 total number of broad groups

```

...space related edit information...

```

24752 number of points to edit
0 number of zones to edit
0 0/1 no/yes density factors were input

```

run highlights

```

*
* all modules are tentatively go.
* interface file goodst written.
* cross sections from cards via bxslib.
* interface mixing files written.
* interface file asgmt written.
* xs files macrxs, srxedt written.
* *left boundary condition overridden*
* interface file soling written.
* interface file editit written.
* start solver execution.
*
* some acceleration inhibition *
* all convergence criteria met.
* interface file rflux written.
* interface file smoms written.
* start edit execution.
* edits completed.
*

```

storage and timing history

module	words	limit	sum	limit	sum	sec	limit	sum	sec
0	0	0	0	0	0	29257.9	0.0	0.0	0.0
100	28971	1100000	0	0	0	24.3	0.0	0.0	0.0
101	0	0	0	0	0	11.6	0.0	0.0	0.0
102	1083	1100000	99	6000000	0.2	0.0	0.0	0.0	0.0
103	438	1100000	0	0	0	0.2	0.0	0.0	0.0
104	2755	1100000	0	0	0	0.3	0.0	0.0	0.0
105	0	0	0	0	0	0.0	0.0	0.0	0.0
106	0	0	0	0	0	0.0	0.0	0.0	0.0
107	2495	1100000	8942	6000000	2.6	0.0	0.0	0.0	0.0
108	0	0	0	0	0	0.1	0.0	0.0	0.0
109	29094	1100000	0	0	0	0.2	0.0	0.0	0.0
112	0	0	0	0	0	0.0	0.0	0.0	0.0
200	638537	1100000	5367012	6000000	29227.8	0.0	0.0	0.0	0.0
201	0	0	0	0	0	28.4	0.0	0.0	0.0
202	0	0	0	0	0	8.3	0.0	0.0	0.0
203	3767	1100000	0	0	0	0.7	0.0	0.0	0.0
204	0	0	0	0	0	0.1	0.0	0.0	0.0
205	0	0	0	0	0	0.2	0.0	0.0	0.0
206	0	0	0	0	0	25457.3	0.0	0.0	0.0
207	0	0	0	0	0	3517.2	0.0	0.0	0.0
208	0	0	0	0	0	0.8	0.0	0.0	0.0
210	0	0	0	0	0	0.4	0.0	0.0	0.0
211	0	0	0	0	0	4.1	0.0	0.0	0.0
300	0	0	0	0	0	5.6	0.0	0.0	0.0
301	150953	1100000	1	6000000	1.9	0.0	0.0	0.0	0.0
302	0	0	0	0	0	0.0	0.0	0.0	0.0
400	0	0	0	0	0	0.0	0.0	0.0	0.0

```

1 tttttttttt hh hh EEEEEEEF 00000000 dddddddddd aaaaaaaaaa nn nn tttttttttt
tttttttttt hh hh EEEEEEEF 00000000 dddddddddd aaaaaaaaaa nn nn tttttttttt
tt hh hh XX XX ee dd dd aa aa aaaa nn nn tt
tt hh hh XX XX ee dd dd aa aa aa nn nn tt
tt hh hh XX XX ee dd dd aa aa aa nn nn tt
tt hh hh XX XX ee dd dd aa aa aa nn nn tt
tt hh hh XX XX ee dd dd aa aa aa nn nn tt
tt hh hh XX XX ee dd dd aa aa aa nn nn tt
tt hh hh XX XX ee dd dd aa aa aa nn nn tt
tt hh hh XX XX ee dd dd aa aa aa nn nn tt
tt hh hh XX XX ee dd dd aa aa aa nn nn tt
tt hh hh XX XX ee dd dd aa aa aa nn nn tt

```

```

0000000 355555555555 2222222222 44 9999999999 3333333333
00000000 355555555555 222222222222 444 999999999999 333333333333
00 00 55 22 444 99 33
00 00 55 22 44 44 99 33
00 00 55 22 44 44 99 33
00 00 55 22 44 44 99 33
00 00 55 22 44 44 99 33
00 00 55 22 444444444444 99 33
00 00 55 22 44 44 99 33
00000000 355555555555 222222222222 44 999999999999 333333333333
0000000 355555555555 222222222222 44 999999999999 333333333333

```

```

PPPPPPPPPP EEEEEEEF 00000000 dddddddddd uu uu aaaaaaaaaa tttttttttt
PPPPPPPPPP EEEEEEEF 00000000 dddddddddd uu uu aaaaaaaaaa tttttttttt
PP XX XX ee dd dd uu uu aa aa aa tt
PP XX XX ee dd dd uu uu aa aa aa tt
PP XX XX ee dd dd uu uu aa aa aa tt
PPPPPPPPPP EEEEEEEF 00 00 dd dd uu uu aa aa aa tt

```

REFERENCES

- Alcouffe, R.E., F.B. Brinkley, D. R. Marr, and R. D. O'Dell, "Revised User's Manual for ONEDANT; A Code Package for ONE-Dimensional, Diffusion-Accelerated, Neutral-Particle Transport", LA-9184-M, Los Alamos National Laboratory (December, 1982).
- Alcouffe, R.E., F.B. Brinkley, D. R. Marr, and R. D. O'Dell, "User's Manual for TWODANT; A Code Package for TWO-Dimensional, Diffusion-Accelerated, Neutral-Particle Transport", LA-10049-M, Rev., Los Alamos National Laboratory (February, 1990).
- Anderson, R.E., Unpublished MCNP Input for SHEBA II, 1990.
- Anderson, R. E., and R. R. Paternoster, Unpublished Draft; "The Solution High-Energy Burst Assembly (SHEBA) Experiments".
- Briesmeister, J. F., "MCNP - A General Monte Carlo Code for Neutron and Photon Transport", V3A, Los Alamos Scientific Laboratory (1986).
- Carter, L. L., and E. D. Cashwell, "Particle-Transport Simulation with the Monte Carlo Method", Los Alamos Scientific Laboratory (1975).
- Clark, B. A., "ONEDANT, TWODANT, and THREEDANT: Application to Criticality Safety Problems", Nuclear Criticality Technology Safety Project Workshop, Monterey, California (April 1993).
- Duderstadt, J.J., and L. J. Hamilton, Nuclear Reactor Analysis, New York: John Wiley & Sons (1976).
- Hansen, G. E., and W. H. Roach, "Six and Sixteen Group Cross Sections for Fast and Intermediate Critical Assemblies", LAMS-2543, Los Alamos Scientific Laboratory (December 6, 1961).
- Lamarsh, J. R., Introduction to Nuclear Reactor Theory, Reading, Mass.: Addison-Wesley Publishing Co. (1966).
- Kornreich, D.E., Unpublished, "summarization of MCNP and TWODANT supporting calculations for the SHEBA-II critical solution assembly" (August 9, 1991).

This report has been reproduced directly from the best available copy.

It is available to DOE and DOE contractors from the Office of Scientific and Technical Information, P.O. Box 62, Oak Ridge, TN 37831. Prices are available from (615) 576-8401.

It is available to the public from the National Technical Information Service, US Department of Commerce, 5285 Port Royal Rd., Springfield, VA 22161.

Los Alamos
NATIONAL LABORATORY

Los Alamos, New Mexico 87545